Contents lists available at ScienceDirect

NeuroImage

journal homepage: http://ees.elsevier.com

Face-sensitive brain responses in the first year of life

Stefania Conte [a,*], John E. Richards [a], Maggie W. Guy [b], Wanze Xie [c,d], Jane E. Roberts [a]

[a] Department of Psychology, University of South Carolina, United States
[b] Department of Psychology, Loyola University Chicago, United States
[c] Laboratories of Cognitive Neuroscience, Division of Developmental Medicine, Boston Children's Hospital, United States
[d] Department of Pediatrics, Harvard Medical School, United States

ARTICLE INFO

Keywords
Event-related potentials
Face processing
Attention
Infancy

ABSTRACT

Cortical areas in the ventral visual pathway become selectively tuned towards the processing of faces compared to non-face stimuli beginning around 3 months of age and continuing over the first year. Studies using event-related potentials in the EEG (ERPs) have found an ERP component, the N290, that displays specificity for human faces. Other components, such as the P1, P400, and Nc have been studied to a lesser degree in their responsiveness to human faces. However, little is known about the systematic changes in the neural responses to faces during the first year of life, and the localization of these responses in infants' brain. We examined ERP responses to pictures of faces and objects in infants from 4.5 months through 12 months in a cross-sectional study. We investigated the activity of all the components reported to be involved in infant face processing, with particular interest to their amplitude variation and cortical localization. We identified neural regions responsible for the component through the application of cortical source localization methods. We found larger P1 and N290 responses to faces than objects, and these components were localized in the lingual and middle/posterior fusiform gyri, respectively. The amplitude of the P400 was not differentially sensitive to faces over objects. The Nc component was different for faces and objects, was influenced by the infant's attentional state, and localized in medial-anterior brain areas. The implications of these results are discussed in the identification of developmental ERP precursors to face processing.

1. Introduction

The brain areas responsible for face processing are well established in adult research but their development during infancy is not well understood. The aim of the present study was to systematically outline developmental changes in infants' cortical responses to faces within the first year of life. We combined data from multiple studies conducted in our lab, which utilized similar methods to investigate event-related potential (ERP) responses to faces and objects (i.e. toys, houses) in typically-developing infants from 4.5 to 12 months of age (Conte and Richards, 2019; Guy et al., 2018; Guy et al., 2016; Richards, 2015; Xie and Richards, 2016). One goal was to analyze developmental changes in the amplitude of ERP components often examined in studies of infant face processing (i.e., P1, N290, P400, Nc). A second goal was to identify brain areas responsible for the generation of ERP components associated with face processing, using source analysis techniques with realistic, age-appropriate head models.

The N170 ERP component has been closely linked to the processing of faces in adults. Greater N170 amplitude is observed in response to faces than non-face stimuli, including objects and houses (e.g., Bentin et al., 1996; Caldara et al., 2003; Carmel and Bentin, 2002; Itier et al., 2006; Itier and Taylor, 2004a,b; Rossion et al., 2000), attended than unattended peripherally presented face stimuli (Eimer, 2000b), inverted than upright faces (Rossion et al., 2000), but not to inverted versus upright objects (Bentin et al., 1996). For these reasons, it is hypothesized that the N170 reflects the structural encoding of configural information in face perception (Bentin et al., 1996; Eimer, 2000a; Rossion et al., 2000).

"Cortical source analysis" incorporates the electrical activity on the scalp and structural neuroimaging information to estimate neural generators of scalp-recorded ERP components. A number of brain areas have been implicated in the generation of the adult N170 (see Table 4 in Richards et al., 2018). The majority of studies conclude that the N170 component is generated primarily in the fusiform gyrus (particularly the middle and posterior fusiform gyri; Deffke et al., 2007; Gao et al., 2019; Rossion et al., 2003; Shibata et al., 2002). The fusiform gyrus is also the brain area most frequently found to be closely associated with face processing studies using fMRI (Berman et al., 2010; Deffke et al., 2007; see Fig. 7 in Gao et al., 2019; B. Rossion et al., 2003). However, some source analysis studies show

* Corresponding author.
E-mail address: contes@mailbox.sc.edu (S. Conte)

https://doi.org/10.1016/j.neuroimage.2020.116602
Received 8 October 2019; Received in revised form 1 Febraury 2020; Accepted 1 Febraury 2020
Available online xxx
1053-8119/

that other areas may play a role in the generation of the N170 (see Table 4 in Richards et al., 2018).

Infants show face-sensitive ERP responses as early as 3 months of age (de Haan and Nelson, 1999; M. W. Guy et al., 2018; M. W. Guy et al., 2016; Peykarjou and Hoehl, 2013; Xie and Richards, 2016). The ERP components elicited by faces, ordered by their temporal sequence, are the P1, N290, P400, and Nc. The P1 is the first positive-going component elicited by visual stimuli. Its peak is observed at occipital electrodes and has been shown to be greater in amplitude at medial than lateral electrodes (Farroni et al., 2002). It is often overlooked in ERP studies on face processing in infancy, because variation in P1 amplitude in adults is believed to reflect changes in low-level visual cues (Rossion and Jacques, 2008; Regan, 1989). The P1 has been investigated in at least three studies of face processing in young infants, and no differences have been observed in amplitude or latency to faces versus non-face objects (Peykarjou and Hoehl, 2013), upright versus inverted faces (Peykarjou and Hoehl, 2013), and intact versus scrambled faces (Macchi Cassia et al., 2006; Parise et al., 2010). Cortical source analysis has been used in adults to localize the P1 component to the striate and extra-striate visual cortex (Di Russo et al., 2002). No study has defined the cortical source of the P1 ERP response to faces in developmental populations.

The second ERP component elicited by face stimuli is the N290. The N290 is the most frequently studied ERP component elicited by faces in infants (de Haan et al., 2003; Halit et al., 2004; Halit et al., 2003; Hoehl and Peykarjou, 2012; Luyster et al., 2014; Luyster et al., 2011). It is a negative-going deflection in the ERP, peaking approximately 290 ms after stimulus onset at lateral-inferior posterior scalp areas (de Haan et al., 2003; M. W. Guy et al., 2016; Halit et al., 2003). Like the adult N170, greater N290 amplitude has been observed in response to human faces than non-face stimuli in infants (M. W. Guy et al., 2018; McCleery et al., 2009; Xie and Richards, 2016). Studies have also reported an effect of stimulus type on N290 latency (i.e., shorter responses to human faces than objects or non-human faces: Halit et al., 2003; McCleery et al., 2009; and null stimulus type effects at the level of the N290 response: de Haan and Nelson, 1999). The responsiveness of the N290 to faces may be modulated by infants' attentional status, as evidenced by a greater amplitude response to faces than toys during periods of attentiveness (and greater amplitude responses during attention than inattention; Guy et al., 2016). Additionally, the N290 may be sensitive to face salience or familiarity, as it has been shown to be greater to own-than other-species faces in infants at least 3 months of age: de Haan et al. (2002); Halit et al. (2003), own-than other-race faces at 9 months of age: Balas et al. (2011), and female than male faces in 7-month-old infants raised by a female caregiver: Righi et al. (2014). However, one study reported no differences in N290 amplitude in response to infant participants' mothers' faces and favorite toys relative to novel female faces and toys (Guy et al., 2016). Similar to the adult N170, increased N290 amplitude is observed for inverted versus upright human faces at 12 months (Halit et al., 2003), but not at younger ages (de Haan et al., 2002; Halit et al., 2003). These results indicate that the N290 reflects infant encoding of faces, and may become more similar to the adult N170 with age.

Cortical source analysis of the infant N290 reveals similar sources to the adult N170. The fusiform gyrus, right STS and surrounding temporal lobe areas have been reported to discriminate upright to inverted faces at 3 and 12 months of age (Johnson et al., 2005). More recently, Guy et al. (2016) showed that the brain areas that show cortical source responsiveness within the time window of the N290 ERP component were the middle fusiform gyrus, anterior fusiform gyrus, parahippocampal gyrus, and temporal pole. Further, the fusiform gyrus along with the inferior occipital gyrus have been identified as generators of the N290 during the discrimination of emotional valence of faces in 5- and 7-month-old infants (Xie et al., 2019). These results indicate that both structural and emotional encoding of faces at the level of the N290 component in the first year of life involve activity of similar cortical areas to the brain areas generating the N170 in adults.

There are variations in the pattern of response to faces and non-face stimuli in mid-latency infant ERP components, including the P400 and Nc. The P400 is most prominent over posterior and lateral electrodes (de Haan et al., 2002; Halit et al., 2003), whereas the Nc is prominent over frontal and central electrodes. The P400 and Nc have an opposite polarity, i.e., positive deflection for the P400 and negative deflection for the Nc. The P400 peaks at approximately 400 ms following stimulus onset, and the Nc is observed from approximately 300 to 800 ms without a strictly defined peak latency (for review see de Haan et al., 2003; Reynolds and Richards, 2005, 2009). The role of the P400 in face processing is somewhat ambiguous. One study reported shorter latency responses to faces than toys in 6-month-old infants (de Haan and Nelson, 1999). However, this effect was not replicated in another study, which reported greater P400 amplitude in response to objects than faces (Guy et al., 2016). Additionally, results of two studies indicate that the P400 activity is modulated by face inversion and shows substantial changes in the first year of life. Specifically, both 3- and 6-month-old infants show larger P400 responses to upright compared to inverted faces, including human and monkey faces (de Haan et al., 2002; Halit et al., 2003). By 12 months of age the P400 shows greater specialization, evident by longer latency responses to inverted than upright human faces, but not inverted and upright monkey faces (Halit et al., 2003). Greater amplitude in the P400 responses have been observed during HR-defined periods of attention than inattention (Guy et al., 2016). Additionally, it is possible that the P400 plays a role in novelty detection, as greater amplitude responses have been reported to novel than familiar faces in some studies (Key et al., 2009; Scott and Nelson, 2006; Scott et al., 2006), but not others (de Haan and Nelson, 1999; Guy et al., 2016). It is often suggested that the mature N170 found in adults may result from an integration of the N290 and P400 with changes in age from 12 months and beyond, since both the N290 and the P400 show analogous structural and functional characteristics to the adult N170 ERP component (de Haan et al., 2003; Halit et al., 2003, 2004; Hoehl and Peykarjou, 2012; Luyster et al., 2011).

The Nc is the most frequently studied ERP component in infancy. It is observed in response to stimuli in almost all modalities and to a number of stimulus conditions. The Nc is frequently shown to be sensitive to stimulus familiarity (Carver et al., 2003; de Haan and Nelson, 1999; C. A. Nelson and Collins, 1991, 1992; Reynolds and Richards, 2005), emotional information (de Haan et al., 2004; Grossmann et al., 2006; Leppanen et al., 2007; Martinos et al., 2012; C. A. Nelson and de Haan, 1996; Quadrelli et al., 2019; W. Xie et al., 2019), and allocation of attentional processing resources (Ackles and Cook, 2007, 2009; de Haan et al., 2007; Dennis et al., 2009; Charles A. Nelson, 1994; Reynolds and Richards, 2005; Richards, 2003). The amplitude of the Nc is larger during HR-defined periods of attention than inattention (Guy et al., 2016; Reynolds et al., 2010; Reynolds and Richards, 2005, 2009; Richards, 2003). The Nc appears to be a generic ERP component reflecting attentional engagement and showing similar responses to the P300 component in adults (Riggins and Scott, 2019). Thus, it often shows responsiveness to face stimuli mirroring the attentional valence of the face stimuli. Infant ERP studies utilizing face stimuli have reported greater Nc responses to infants' mother's face than dissimilar looking stranger's face in 6-month-olds (de Haan and Nelson, 1997, 1999; Webb et al., 2005). It is modulated by the relative salience of the face (Courchesne et al., 1981; de Haan and Nelson, 1997, 1999; Maggie W. Guy

et al., 2013; Reynolds et al., 2010; Richards, 2003; Webb et al., 2005).

Source location of the Nc component in infant participants has been investigated in response to face and non-face stimuli. Reynolds and Richards (2005) examined the cortical source of the Nc component in response to computer-generated visual patterns with and without previous familiarization exposure during a modified-oddball procedure. They reported that the Nc amplitude increased with infants' attentional status and preference for novel stimuli. By 7.5 months of age, generators of the Nc responses were mainly localized in areas of the inferior prefrontal cortex and anterior cingulate cortex (Reynolds and Richards, 2005; also see Reynolds et al., 2010). Guy et al. (2016) localized the Nc, measured in response to faces and toys, in the anterior temporal lobe and prefrontal cortex in infants at 4.5–7.5 months of age. Activity of the Nc in response to emotional faces has been localized to posterior sources, e.g., posterior cingulate cortex/precuneus (Xie et al. 2019). The discrepancy between these studies may be due to the differences in the stimuli utilized – familiar versus unfamiliar face and toy stimuli in Guy et al. (2016) and emotional faces in Xie et al. (2019). It is possible that the time window considered for source analysis of emotional stimuli included a combination of a distinct P400 source overlaid on the beginning of the Nc source, resulting in the localization of the component in posterior rather than central-inferior sources. The P400 and Nc share a similar latency and a dipolar appearance of scalp activation, which makes it difficult to determine unique sources for each component during face processing (Guy et al., 2016).

In summary, extensive research has been conducted to characterize infants' face-specific ERP responses. However, these studies have generally examined face processing at one or two specific ages and not over the entire first year. These studies often compare face-related stimuli across categories (familiarity; species effects; ethnicity) and not specifically to non-face stimuli. The current study examined the development of electrophysiological responses to faces and objects in the first year of life. The ERP activity was examined in a cross-sectional design with infants from 4.5 to 12 months of age (Conte and Richards, 2019; Guy et al., 2016, Guy et al., 2018; Richards, 2015; Xie and Richards, 2016). The primary goal was to systematically track infants' neural responses to faces and non-face objects in the first year of life and modulated by attention. Several studies have used heart rate deceleration during stimulus presentation as an index of attention or arousal in infants. Infant processing of stimulus information occurs primarily during periods of sustained attention (Reynolds and Richards, 2007; Richards, 2001; Richards and Casey, 1992; Richards et al., 2010). It has been shown in several studies that ERP responses to stimuli, including faces, are larger and more organized during HR-defined sustained attention then during inattention (Guy et al., 2016; Reynolds and Richards, 2005; Richards, 2003; Xie and Richards, 2016) These studies also found that significant differences in the ERP response occurred for age and stimulus conditions during attention but not during inattention. We hypothesized that larger amplitude responses to faces compared to objects would be elicited during early stages of processing (i.e., P1 and N290), whereas later components (i.e., P400 and Nc) would be modulated by attentional processes.

A second aim of this study was to localize the cortical generators of infant face-sensitive ERP components and to examine changes in their sources across the first year of life. We used source localization methods that included realistic head models based on individual MRIs and age-appropriate infant templates. We applied a voxel wise segmentation of all relevant head materials, utilized finite element method (FEM) procedures for the source analysis, and considered a series of regions of interest (ROIs) in the ventral temporal-occipital pathway typically linked to face processing (Gao et al., 2019; Guy et al., 2016; Richards et al., 2018). Previous research has shown that the N290 is generated in the fusiform gyrus (Guy et al., 2016; Johnson et al., 2005), but the localization of the P400/Nc components has been less clear. We predicted that early ERP responses, such as the P1, would reflect the activation of those areas defined as occipital face areas in fMRI studies with adults (i.e., lateral inferior occipital gyrus; Bernstein and Yovel, 2015), the fusiform gyrus would be the source of the N290 response for faces, whereas the activation of both the P400 and Nc in response to faces would be modulated by infants' allocation of attention and localized in the posterior cingulate cortex and anterior cingulate and prefrontal cortex, respectively (Richards et al., 2010; W. Xie et al., 2019).

2. Material and methods

2.1. Participants

One hundred and thirty-two infants were included in the final sample and recruited from the Columbia, SC metropolitan area using birth lists that were purchased from INFO USA (Omaha, NE). All infants were full term (at least 38 weeks gestation, birth weight at least 2500 g) and healthy at birth with no known developmental anomalies. Participants were primarily Caucasian and of middle socioeconomic status. The recruitment strategy for the experiments involved recruiting participants at 4.5, 6, 7.5, 9, and 12 months. However, there were fewer participants at 7.5 and 9 months. Therefore, we combined participants from those to homes and used four separate age groups of 4.5, 6, 8, and 12 months.[1] Table 1 reports demographical information of participants included in the current study. Details of attrition due to fussiness or procedural error can be found in articles by Guy et al. (2016, 2018 and Xie and Richards (2016). Informed parental con-

Table 1
Demographical information of participants included in the final sample for each age group.

Age group	Sample size	N. of male participants	Average age in days (SE)	N. of participants per experiment
4.5 months	37	21	147.89 (1.77)	Guy et al. (2016) n = 17 Xie and Richards, 2016 n = 13 Conte and Richards, (2019) n = 7
6 months	39	20	191.38 (1.30)	Guy et al. (2016, 2018 n = 20 Xie and Richards, 2016 n = 13 Conte and Richards (2019) n = 6
8 months	21	12	247.90 (6.21)	Guy et al. (2016) n = 13 Richards, unpublished n = 8
12 months	35	26	377.40 (2.26)	Guy et al. (2016, 2018 n = 24 Conte and Richards (2019) n = 11

sent was obtained in accordance to ethics approval from the Institutional Review Board of University of South Carolina.

2.2. Stimuli

The stimuli consisted of pictures of faces and objects (i.e., toys and houses) presented on variegated backgrounds containing simple stimuli (i.e., water, sand, clouds or grass). Faces and objects were presented on an LCD monitor subtending approximately 13 × 17 degrees of visual angle. There were three procedures used in the studies. We considered the trials in which faces and objects were centrally presented on the screen. The stimuli in Guy et al. (2016, 2018 and Richards (2015) consisted of single central presentations one image at a time from four images (i.e., two faces and two toys) created from photographs of a woman's face and a toy. The images were digitized photographs of the participant's mother's face, participant's toy, and photographs of the mother's face and toy from the previous participant. The stimuli in Xie and Richards, 2016 consisted of 12 faces taken from the NimStim database (Tottenham et al., 2009) and 12 toys from the Guy et al., 2018 study. The same subset of faces used in Xie and Richards, 2016 were compared to pictures of 12 houses with symmetrical features in Conte and Richards (2019; upright faces and upright houses only). Example of the stimuli can be found in Supplementary Fig. 1.

2.3. Apparatus and procedure

Participants were seated on their parent's lap, 55 cm away from a 29″ LCD monitor (Hanns.G HG281D) in a darkened and sound-attenuated room. A video camera positioned above the monitor recorded the participant's face. In an adjacent room, an experimenter viewed the infant on a TV monitor while controlling the stimulus presentations using an E-Prime experiment program.

Fig. 1 (panel A) depicts the three experimental procedures and examples of stimuli used in the current study. A moving video of Sesame Street characters was presented in the center of the screen, under an area of 2 × 3 degrees of visual angle, to attract the infant's fixation to the monitor. After the infant had fixated on the center of the screen, the experimenter began the trial by pressing a button. In Guy et al. (2016, 2018) this was followed by a sequence of brief image presentations and paired comparison (PC) trials. Faces and toys were presented for 500 ms, followed by a variable inter-trial interval of 500–1500 ms. We did not consider the data from the PC trials for the current analysis. Xie and Richards, 2016 presented the stimuli for 500 ms using random without replacement presentation sequences[2]. Conte and Richards (2019) presented faces and houses randomly without replacement for 500 ms, followed by a variable inter-trial interval of 500–1000 ms.

An experimenter monitored the infant's fixations toward the screen. If the infant looked away a moving Sesame Street character was presented to draw his/her fixation back toward the screen. A digital recording of the video was used to confirm offline that the infant was looking at the stimulus during the brief stimulus presentations. Trials were only included in the analyses if the participant looked the entire time without eye movements.

2.4. Recording of ECG and heart-rate defined attention

The electrocardiogram (ECG) was recorded with two Ag–AgCl electrodes placed on infants' chests. These were digitized along with EEG using the EGI (Electrical Geodesics Incorporated, Eugene, OR) 128-channel EEG recording system (Johnson et al., 2001; Tucker, 1993). The ECG was analyzed offline to assess changes in HR to define periods of attention and inattention in a continuous presentation method (Mallin and Richards, 2012; Pempek et al., 2010; Reynolds et al., 2010). During periods of attention, the infant was looking toward the screen and showed both a deceleration in HR below the pre-stimulus level (five beats with inter-beat intervals (IBIs) > median pre-stimulus IBIs) and sustained lowered HR (IBIs > pre-stimulus median). Inattention was defined as when the infant looked toward the screen, but the HR deceleration had not yet occurred, or the infant continued looking toward the screen after the lowered HR returned to pre-stimulus levels. Inattention continued until another significant HR deceleration occurred. If the infant looked away the attention phase was undefined, and then the sequence began again when the infant looked back toward the screen.

2.5. Recording and segmenting of EEG

Details of the EEG recording can be found in Guy et al. (2016, 2018 or Xie and Richards, 2016. The EEG was recorded using the EGI 128-channel EEG recording system. Participants were fitted with either a "geodesic sensor net" (GSN) or "hydrocel geodesic sensor net" (HGSN), with the net circumference matching the infant head circumference. The EEG was measured from 124 channels in the electrode net and two channels over the outer canthi for electrooculogram (EOG). Impedances of less than 100 kΩ were attained before each recording commenced and a 0.1–100 Hz band-pass filter was applied during the recordings. The vertex-referenced EEG was algebraically recomputed to an average reference.

The EEG recordings were processed with the EEGLAB (version 14.1.1b) and ERPLAB toolboxes (Delorme and Makeig, 2004; Lopez-Calderon and Luck, 2014) within MATLAB R2019a. Computational and visual artifact rejection methods were used to detect and eliminate bad channels on individual trials. The bad channels were substituted with data from the five closest electrodes proportional to the distance of the bad channel to the substituted channels. The trial was rejected if it contained 12 or more bad channels. Infants viewed an average of 117 trials (4.5 months: $M = 139$; 6 months: $M = 124$; 8 months: $M = 83$; 12 months: $M = 103$). The number of trials contributing to the analyses consisted of a minimum of 10 trials per condition. Further details about the average number of trials in each condition and age group are reported in Table 2.

2.6. ERP data analysis

The electrode map in Fig. 1 (panel B) shows both electrode location and electrodes used for the data analysis. Studies of face processing in infants typically use single electrodes from the 10–20 or 10-10 system for their analyses (Courchesne et al., 1981; Karrer et al., 1998), clusters of electrodes recording from 10 to 20 or 10-10 recording electrodes (de Haan and Nelson, 1999), and more recently use electrode clusters from the EGI 64- or 128-channel system intended to represent 10-10 electrode positions (Luyster et al., 2014; Scott and Nelson, 2006). The EEG data in the current study from the 126 electrodes were translated into 81 "virtual 10-10" channels using a spherical spline interpolation from the 126 channel locations to the 81 channel locations. The EGI-126 channel data were used for topographical scalp potential maps and source analyses. The 10-10 channel data were used for single-electrode ERP plots and analyses.

The EEG was re-referenced to the to the algebraic mean of all channels and segmented from 100 ms before stimulus onset through 1000 ms following onset. The EEG was filtered with a 0.5–35 Hz bandpass filter for the N290, P400, and Nc ERP components, whereas a 1–35 Hz bandpass filter was used for the P1. Fig. 1B (bottom panels) depicts grand average ERP responses to faces and objects, and HR-defined periods of attention to faces and objects as a function of time and separately for age group. The ERP activity of 7.5- and 9-month-old infants are plotted separately in order to show how at 9 and 12 months the pattern of responses to faces resembles each other.

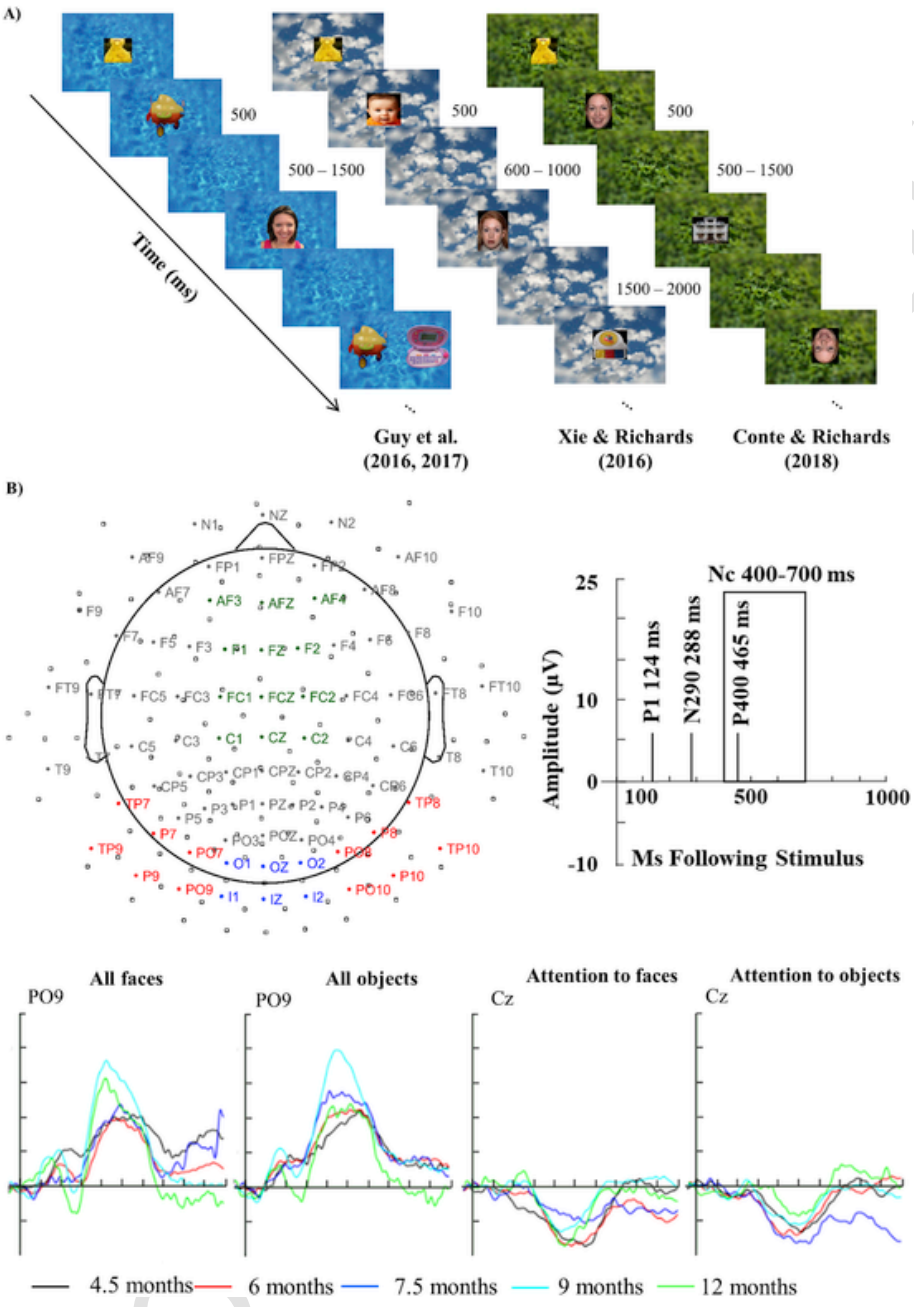

Fig. 1. From left to right panel A shows a schematic representation (not drawn in scale) of the procedures reported in Guy et al. (2016, 2018 , Xie and Richards, 2016, and Conte and Richards (2019). Of note, only stimuli presented in the center of the screen and with upright orientation were considered for analysis in the current work. Panel B displays a topographic map of channel locations from EGI 128-channels (empty dots) used for data recording, and 10-10 system (filled dots) used for data analysis. The channels we used as ROIs for ERP analyses are marked with colors; Blue channels were used to analyze the P1 activity (medial inferior-posterior ROI), red channels were considered for the N290 component (lateral inferior-posterior ROIs), green channels in the fronto-central area were grouped to analyze the Nc ERP component, and a sub-set of inferior-posterior channels (P7, P9, PO7, PO9, O1, Oz, Os, I1, Iz, I2, PO8, PO10, P8, P10) defined the ROI for the P400 component. ERP line graphs show the grand average ERP response across age groups for faces and objects at PO9 and for attention to faces and objects at Cz. (For interpretation of the references to color in this figure legend, the reader is referred to the Web version of this article.)

Amplitudes of the P1, N290, and P400 were measured by calculating the change in amplitude between the peak of the component of interest and the peak of the preceding component using ERP averages from each participant. Peak-to-trough differences were calculated between the P1 peak and the preceding negative peak at medial inferior posterior electrodes (median from peaks at Oz, O1, O2, Iz, I1, I2). Individual ERP averages were manually inspected to identify the peak of the P1. If no peak was obvious, we completed the peak-to-trough analysis using the P1 value at 100 ms (Xie and Richards, 2016). The N290 peak amplitude was selected from individual participants' ERP averages and defined as the most negative value observed between the peak of the P1 ERP component and 400 ms at lateral inferior posterior electrodes (i.e., median from peaks at PO7, PO8, PO9, PO10, P7, P8, P9, P10, TP7, TP8, TP9, and TP10). Similarly, the P400 peak amplitude was defined as the most positive peak between the N290 peak and 700 ms after stimulus onset at medial inferior posterior electrodes (i.e., median from peaks at Oz, O1, O2, Iz, I1, I2, PO7, PO8, PO9, PO10, P7, P8, P9, and P10). If no peak was obvious in the manual inspection, an average latency of each component was used to extract the ERP amplitude. Peak-to-trough differences were calculated between the P1 and preceding negative peak, the N290 and preceding positive peak (i.e. P1), and the P400 and the preceding negative peak (i.e. N290) to con-

Table 2
For each category the average number of trials considered for the analyses is reported across ages.

	Faces	Objects	Attention to Faces	Attention to Objects	Inattention
4.5 months	32.14	31.39	21.57	18.80	42.83
6 months	30.68	31.08	18.85	19.03	40.22
8 months	37.52	37.57	20.29	19.93	42.81
12 months	31.19	30.65	23.68	23.00	43.65

trol for the potential effect of slow waves (Conte et al., 2019; Guy et al., 2016; Kuefner et al., 2010; Peykarjou et al., 2013). Statistical analyses focused on the amplitude values of the 10 ms surrounding the peaks identified in the individual ERP averages for the P1, N290 components, and the 40 ms surrounding the peak of P400 component. The Nc amplitude was defined as the mean amplitude from 400 to 700 ms following stimulus onset at medial frontal-central electrodes (i.e., AFZ, AF3, AF4, FZ, F1, F2 FCZ, FC1, FC2, CZ, C1, and C2).

Stimulus type (2: faces, objects) and attention type (3: attention-faces, attention-objects, inattention) factors were analyzed separately for all ERP components. We combined the response to faces and objects during inattention as a single level in the design because the we did not expect to find differences in the response to faces and objects during inattention (Guy et al., 2016, 2018). Significant ERP effects were further investigated utilizing the source analysis procedure to determine the source localization of ERP responses to faces.

2.7. Cortical source analysis

Cortical source analysis of the ERP components was conducted with the Fieldtrip (FT; Oostenveld, Fries, Maris and Schoffilen, 2011) computer programs and in-house custom MATLAB scripts. The cortical source analyses focused on data around the peaks identified in the individual ERP averages for the P1, N290, and P400 components (±10 ms for the P1 and N290 and ±40 ms for the P400), and data from the entire 400–700 ms period after stimulus onset for the Nc. Detailed information about the source analysis may be found in Guy et al. (2016), and Gao et al. (2019) and in the Supplemental Information documents accompanying those publications (e.g., Appendix S1 in Guy et al., 2016; Richards et al., 2018).

We used realistic head models based on individual participant structural MRIs and electrode placements. Seventy-two of the infants (54%) had a structural MRI from which the head models were used. Sixty infants (46%) did not have a MRI so we selected for those infants an MRI close in head size and age from the Neurodevelopmental MRI Database (Richards et al., 2015; Richards and Xie, 2015). The MRIs were segmented into component materials (gray matter, white matter, CSF, dura, skull, muscle, eyes, nasal cavity, scalp). The segmented MRIs were transformed to wireframes and a finite element method (FEM) head model was generated with source dipoles restricted to the gray matter and eyes. Head models detailing electrode placement were created based on photographs of the electrodes on the participants' heads. Anatomical ROIs were identified in individual MRIs through the use of stereotaxic atlases created for each MRI (Fillmore et al., 2014; Phillips, 2013). Supplementary Fig. 2 shows CDR values around the peak of P1, N290, and P400 across all the anatomical ROIs. The ROIs chosen included the orbital-frontal gyrus, frontal pole, ventral and dorsal anterior cingulate (anterior-medial areas), anterior temporal pole, anterior fusiform gyrus, parahippocampal gyrus (anterior-lateral areas), middle fusiform gyrus, posterior fusiform gyrus, superior temporal gyrus, inferior occipital gyrus lateral, inferior temporal gyrus posterior, lingual gyrus, middle temporal gyrus (mid-posterior lateral areas), posterior cingulate, and superior parietal lobe (posterior-medial areas). Fig. 2 displays the ROIs of the ventral stream of visual processing on a 12-month-old participant's template. The most relevant regions for the processing of faces are presented in color, with particular attention to the portions of the fusiform gyrus. We used the anatomical ROIs used in Gao et al. (2019; see also Richards et al., 2018) to analyze the current density reconstruction (CDR) values across ages.

Current density amplitude in the dipole source (GM and eyes) locations was estimated with the CDR technique and exact-LORETA (Pascual-Marqui et al., 2011)(eLORETA; Pascual-Marqui, 2007; Pascual-Marqui et al., 2011) as the constraint for the CDR technique. The ERP data surrounding the P1, N290, and P400 peaks, and within the Nc time window, were used to estimate the current density amplitudes (i.e., CDR values) for every location in the source volume model. The CDR values were then summed over each source location in a ROI and divided by the total volume of the ROI. This resulted in the aver-

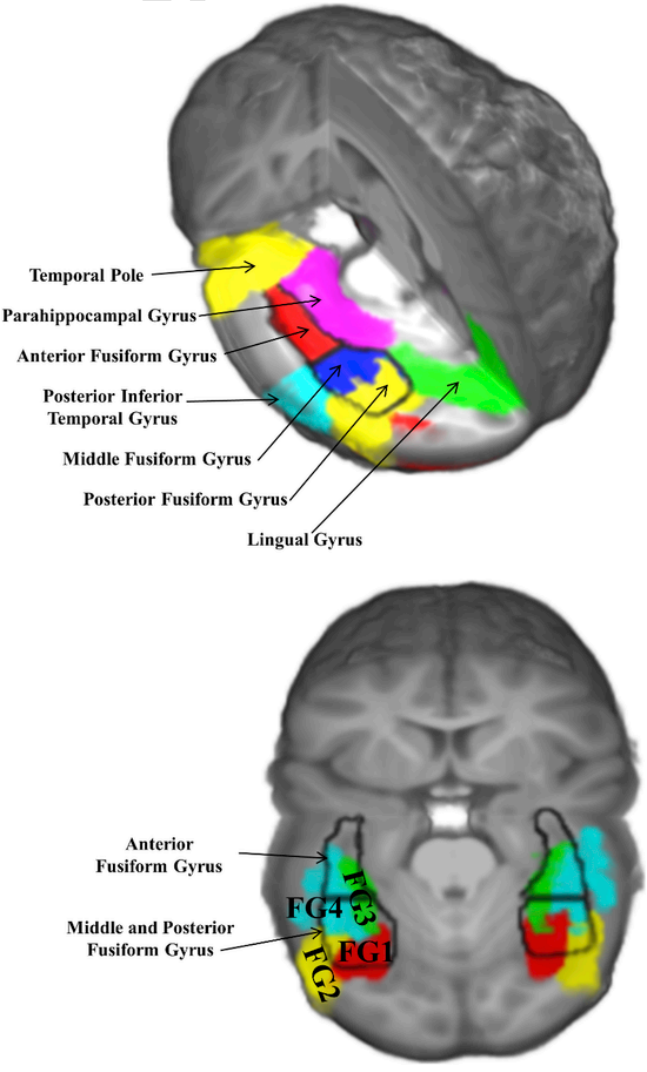

Fig. 2. 3D rendering representation of the ventral surface of temporal and occipital lobes on a 12-month-old average template. Top panel shows the main ROIs utilized to analyze CDR values in response to faces and objects. The theoretically most important region for the face processing is the fusiform gyrus, which is encircled with a black line. Bottom panel depicts ventral occipital temporal ROIs (FG1-4) described in Rosenke et al. (2018) and the fusiform gyri transformed into the average 12-month-old template. Anterior edges of FG1 and FG2 separate the middle and posterior portions of the fusiform gyrus.

age Ampere per mm^3 (A/mm^3) for each ROI. We created simulated MRI volumes by transferring the CDR values for each individual MRI to an age-appropriate average template in addition to the calculation of CDR values for each ROI segment individually, so that the average current density amplitude across participants could be displayed in the average MRI space. More information about using the CDR technique and realistic head models for cortical source analysis can be found elsewhere (Gao et al., 2019; Guy et al., 2016; Richards, 2013; Richards et al., 2018; Xie and Richards, 2016; and Supplemental Information in those articles).

2.8. Design for statistical analyses

Mixed-design ANOVAs were calculated to determine the effects of age, stimulus type, HR-defined attention phase, electrode location, and electrode hemisphere (N290 only) on the P1, N290, and P400 peak amplitude, and the Nc mean amplitude. We explored the amplitude values of all ERP components as a function of both stimulus type (i.e., faces and objects) and HR-defined attention phases (i.e., attention to faces, attention to objects, and inattention) in separate analyses. The design included age (4: 4.5 months, 6 months, 8 months, 12 months) as a between-subjects factor, and stimulus type (2: faces, objects), and electrode location (see Fig. 1, panel B) as repeated measures factors. We also examined the data separately from the 8-months group for 7.5- and 9-month-old participants to see if there were important changes at those two ages. Further, we were interested in investigating whether the infant's attention modulated the neural responses to faces when compared to either objects or periods of inattention. Thus, when the attention was included, we analyzed this as a 3-level repeated measures factor (3: attention to faces, attention to objects, and inattention). We added hemisphere (2: right, left) as an additional within-subjects factor for the N290 only, in order to test the hemispheric lateralization of face-sensitive processes (Halit et al., 2004).

Similarly, the CDR values of each ERP component were analyzed as a function of age, stimulus type, HR-defined period of attention, and ROI. The analyses of cortical sources were done separately for the P1, N290, P400, and Nc components. The data for the analyses were based on the source CDR values calculated from the peak of the ERP components (P1, N290, P400) or a 400–700 ms time-window (Nc). The source analysis transforms the scalp electrodes into anatomical ROIs, so that the statistical analyses were done on CDR values surrounding the peak/time-window of the component with multiple dependent variables from the CDR ROIs. We used a total of 16 ROIs based on previous studies of source analyses for faces in infancy (Guy et al., 2016; Xie et al. 2019) and averaged over activity within bilateral ROIs to control the false-positive rate.

We calculated the effect size of stimulus type and attention type effects at each ROI within their respective brain area (e.g., anterior-medial, anterior-lateral, mid-posterior lateral, and posterior-medial) for each ERP component. We further examined the effects of age, stimulus type, and attention type comparing the CDR values of those regions with a high effect size (i.e., η^2 value) and either a significant or nonsignificant stimulus effect, in order to reduce the number of comparisons.

We used the general linear model approach to ANOVAs with the "Proc GLM" of SAS (version 9.4) using nonorthogonal design (see Searle, 1987). All significant tests are reported at $p < .05$.

3. Results

3.1. P1 ERP component

Fig. 3A shows the ERP responses to faces and objects at each electrode of the medial-inferior posterior cluster in the 12-month-old group (see Fig. 1, panel B for a comparison between age groups). The P1 is evident as a small positive ERP component peaking on average at 124 ms after stimulus onset. Fig. 4A shows the changes in the ERP for faces and objects centered at the peak of the P1 in the topographical maps (top panels), sample-by-sample graphs (middle panels) and with bar charts (bottom panels). Responses to faces and objects were equally large at 4.5 months, but became larger for faces than objects at the following ages.

The peak P1 amplitude was analyzed as a function of stimulus type (faces, objects) and age (4.5, 6, 8, and 12 months), with medial inferior posterior electrodes (Oz, O1, O2, Iz, I1, I2) as multiple dependent variables. The effect of stimulus type (F (1, 15) = 9.16, p = .003) was qualified by a significant interaction between stimulus type and electrode location, F (5, 15) = 2.27, p = .046. No other main effects or interactions were significant. The stimulus type effect reflected a larger P1 response to faces than objects across medial inferior posterior electrodes (Fig. 4A). Univariate ANOVAs were performed at each electrode to further explore the interaction between stimulus type and electrode location. The results revealed a significant stimulus type effect at all of the medial inferior posterior electrodes characterized by larger P1 peaks for faces than objects. The simple effects were further examined through the calculation of effect sizes, which revealed that the variance in responses across stimulus type was largest at the Oz electrode (η^2 = 0.10).

We also examined the effect of the HR-defined periods of attention on the P1 amplitude in a mixed-ANOVA, including electrode location, attention phase (attention-faces, attention-objects, inattention), and age. There was a significant main effect of attention phase, F (2, 180) = 4.45, p = .013. Follow-up comparisons (Bonferroni corrected) showed that the P1 amplitude was greater in response to faces during periods of attention (M = 5.37 μV) than both during inattention (M = 4.27 μV), and in response to objects during attention (M = 4.14 μV), p's < 0.0001.

3.2. Sources of P1 ERP component

Preliminary analysis of CDR values at the peak of the P1 component showed a significant stimulus type effect in the lingual gyrus (LG, p = .0258, η^2 = 0.116) and parahippocampal gyrus (PHG, p = .0381, η^2 = 0.098). The bottom panels of Fig. 4B display the CDR activity around the peak of the P1 for faces separately for the LG, PG, and anterior temporal pole (aTP) ROIs across ages. The aTP is included because it had a large CDR amplitude but nonsignificant stimulus effect (p = .229, η^2 = 0.0350). Both the PHG and aTP show large CDR responses, but only the LG shows a peaked pattern around the P1 ERP peak.

The CDR at the peak of the P1 component for faces and objects was further analyzed with an age by stimulus type mixed-ANOVA including only CDR values from the selected ROIs (i.e., LG, PHG, and aTP) as multiple dependent variables. The results revealed a significant main effect of ROI, F (2, 248) = 5.69, p = .0039, with the highest current density amplitudes in the LG (M = 5.111, SD = 14.846), followed by the PHG (M = 4.195, SD = 12.893) and aTP (M = 3.702, SD = 12.466). The post hoc comparisons (Bonferroni corrected) showed that all the contrasts were significant (p's < 0.0001). There were no other significant main effects or interactions.

The amplitude values around the peak of the P1 were modulated by the HR-defined periods of attention in the ERP analyses. Thus, a preliminary analysis was conducted on attention trials (i.e., attention-faces, attention-objects, inattention) in order to subsequently compare CDR values of ROIs sensitive to attention type. The results showed a significant attention effect at both the aTP (p = .0032, η^2 = 0.176) and middle temporal gyrus (MTG, p = .0091, η^2 = 0.233). Several additional ROIs within the mid-posterior lateral area (i.e., the superior temporal gyrus, lingual gyrus, inferior occipital gyrus lateral, mid-

dle fusiform gyrus, and inferior temporal gyrus posterior, p's < 0.0404) showed a significant attention type effect, but smaller η^2 values, thus these regions were excluded from further analyses. We selected an additional ROI in which we observed large CDR amplitudes but non-significant attention effect, the orbital-frontal gyrus (orbFG, $p = .1276$, $\eta^2 = 0.241$), to include in the comparison.

The analysis of the CDR at the peak of the P1 component was performed with an age by attention type mixed-ANOVA with the CDR values from the selected ROIs (3: aTP, MTG, orbFG) as multiple dependent variables. The results showed significant main effect of both attention type (F (2, 105) $= 25.55$, $p < .0001$) and ROI (F (2, 250) $= 35.46$, $p < .0001$) factors. These main effects were better qualified by a significant interaction between attention type and ROI, F (4, 210) $= 2.43$, $p = .0485$. Univariate ANOVAs calculated for each region revealed significant effects of attention type, F's (2, 110) > 19.96, p's < 0.0001, for all of the included ROIs. The CDR amplitude during attention to faces was larger than CDR amplitude during attention to objects and inattention trials. The aTP had the largest effect size ($\eta^2 = 0.275$).

3.2.1. Summary P1

Face stimuli selectively influenced the activity of the P1 ERP component by eliciting larger P1 peak responses than objects, and this difference tended to increase across age. However, this selective response for faces did not emerge in cortical source analyses when comparing CDR amplitudes in response to faces and objects in the LG, PHG, and aTP. Stimulus type effects on the CDR values were observed when examined in conjunction with HR-defined periods of attention. Greater CDR activation was observed in response to faces during periods of attention than in response to objects during attention and in response to faces or objects during inattention. The effect of attention to faces on CDR activity was strongest in the aTP.

3.3. N290 ERP component

The N290 in response to faces and objects over lateral inferior posterior electrodes at the representative age of 12 months is depicted in Fig. 3B. The N290 appears more peaked and greater in amplitude at medial than lateral electrodes, with an average peak latency of 288 ms after stimulus onset. We noted some differences between 7.5- and 9-month-infants in their pattern of N290 ERP response, so these ages are plotted separately in Fig. 5. Fig. 5A depicts the scalp topographical distribution of ERP activity at the peak of N290 for faces and objects, and across the five age groups (top panels). Sample-by-sample line graphs (middle panels) and bar charts (bottom panels) represent the changes of ERP amplitudes around the N290 peak for faces and objects. The N290 increases in amplitude with increasing age, but only at 9 and 12 months N290 amplitudes do appear peaked and larger for faces than objects. Fig. 5B shows a 3D-rendered topographical scalp potential map of the N290 peak in response to faces at 12 months of age. The group average response is plotted on a 12-months template and compared to the response of four individuals using either a self or close MRI template. There were individual differences in the distribution of the N290 on the scalp, which could reflect differences in the source location of this component or the electrical proprieties of underlying tissues.

The N290 peak amplitude was analyzed with a stimulus type (faces, objects) by hemisphere (right, left) by age (4.5, 6, 8, and 12 months) mixed-ANOVA, with medial inferior posterior electrodes as multiple dependent variables. The main effect of age, F (3, 126) $= 4.17$, $p = .0075$, and the interaction between stimulus type and electrode location, F (11, 120) $= 2.52$, $p = .0038$, were significant. This interaction was further explored by testing with univariate ANOVAs the stimulus effect at each electrode location. The results showed a signifi-

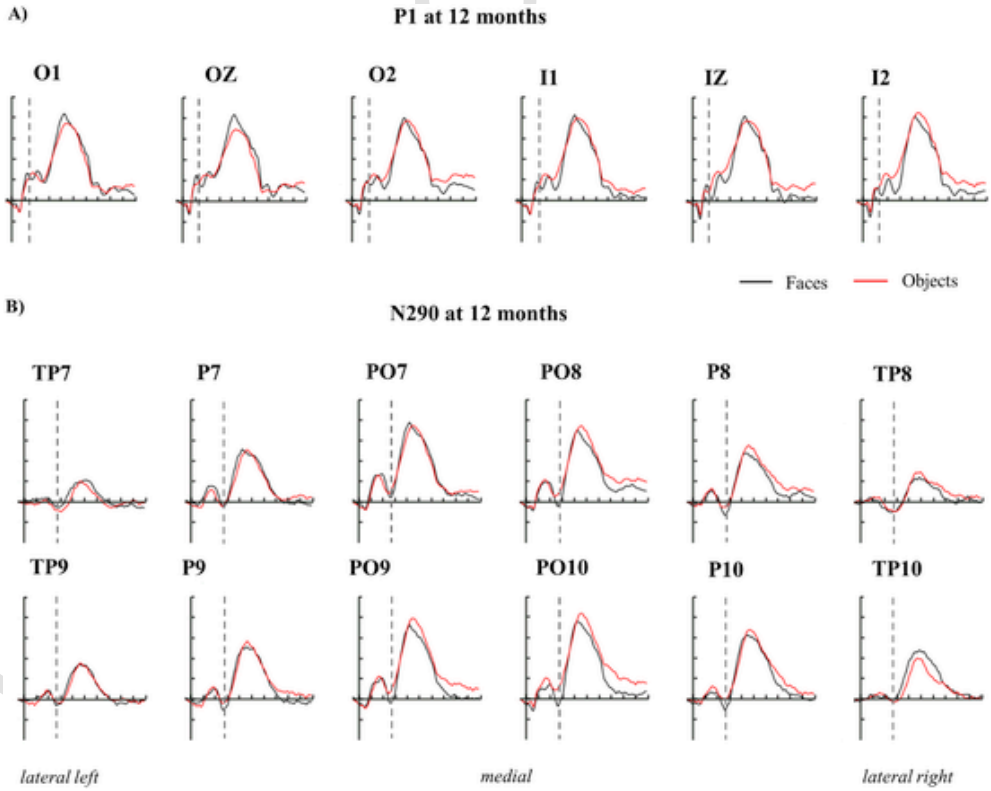

Fig. 3. ERP grand average (−50 to 1000 ms from stimulus onset) for faces and objects of 12-month-old infants. Panel A highlights the ERP activity of the P1 component at each of the inferior occipital channels. In panel B the N290 ERP response is marked in each inferior-lateral occipital-temporal channel. Amplitude ±10 ms around the peak (dotted vertical lines) defined the analyzed ERP values of both P2 and N20 components. Legend of x-axis and y-axis is reported in Fig. 1B.

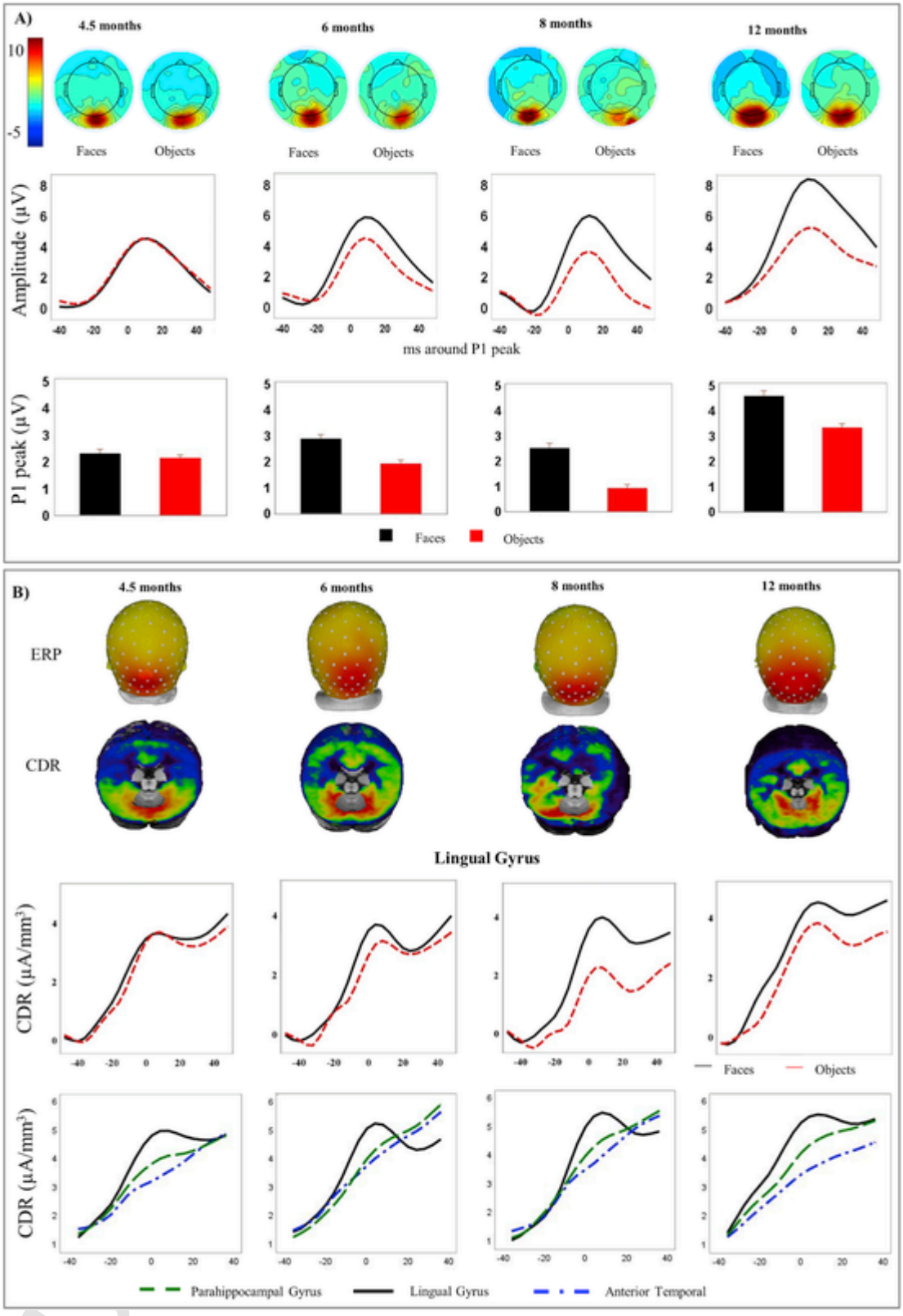

Fig. 4. P1 response to faces and objects over inferior occipital channels across ages. Panel A shows scalp topographical maps at the P1 peak separately for faces and objects (top), ERP amplitude from −40 to +40 ms around P1 peak (middle), and bar graphs of P1 peak for faces and objects over all the ages (bottom). Panel B depicts a 3D rendering of ERP and CDR (coronal cut) responses to faces at the peak of P1 component (first two lines) plotted on the average age-appropriate MRI template. Line graphs display CDR amplitude for faces and objects centered at the peak of P1 (from −40 to +40 ms) separately for the testing ages at the Lingual Gyrus, and CDR values in response to faces at the three analyzed ROIs. The quadratic pattern of activation is visible in both Lingual Gyrus and Posterior Cingulate, but not in the Anterior Temporal pole.

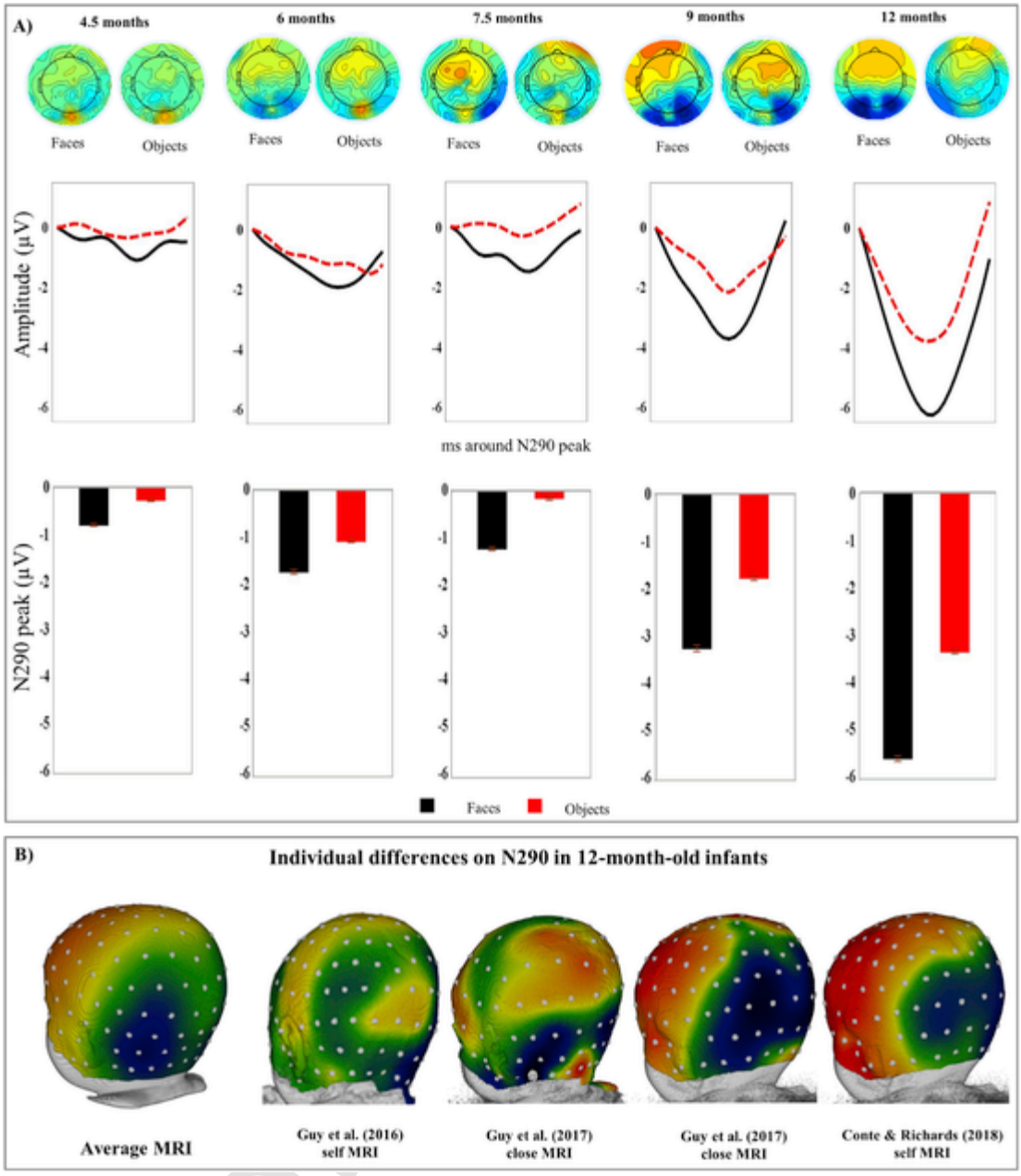

Fig. 5. N290 response to faces and objects over inferior-lateral occipital-temporal channel across the tested ages. Panel A shows scalp topographical maps at the N290 peak separately for faces and objects (top), ERP amplitude from −40 to +40 ms around N290 peak (middle), and bar graphs of N290 peak for faces and objects over all the age groups (bottom). Panel B illustrates the ERP response for faces at the peak of N290 component at 12 months for the average template (leftmost head plot) and four individuals. Individual average response to faces at the N290 peak was superimposed to the individual or the closest MRI volume.

cant stimulus effect at the parietal-occipital electrodes (PO7 through PO10) and some parietal electrodes (P8 through P10; p's < 0.0021), but not at the P7 or temporal-parietal electrodes (p's > 0.8390). The N290 ERP component was larger in amplitude for faces than objects. The simple effects were further examined through the calculation of the effect sizes, which revealed that the stimulus variance was largely explained at parietal-occipital electrodes (PO7 $\eta^2 = 0.046$; PO8 $\eta^2 = 0.063$; PO9 $\eta^2 = 0.065$; PO10 $\eta^2 = 0.074$. See Inline Supplementary Table 1 for all the effect sizes).

The effect of attention on the N290 amplitude was examined in an ANOVA including attention type (attention-faces, attention-objects, inattention), hemisphere, and age as factors, with lateral inferior posterior electrodes as multiple dependent variables. There were no significant effects involving attention type.

3.4. Sources of N290 ERP component

Fig. 6A shows ERP scalp activity for faces and the respective CDR distribution on the age-appropriate MRI template of each age group. There was a larger N290 response to faces with increasing age, which was bilaterally localized in the fusiform gyrus (bordered in black). Note that at 9 months of age, but not 7.5 months of age, both the ERP and CDR patterns of activity in response to faces resembled the infants' neural responses to faces at 12 months.

Similar to the CDR analyses of the P1 component, we performed a preliminary analysis on current density amplitudes around the peak of the N290, in order to select the ROIs to include in the analyses examining age and stimulus type effects. We explored the effect of faces

and objects on the N290 CDR values at each of the 16 ROIs, and found a statistically significant effect at three ROIs within mid-posterior lateral areas (middle fusiform gyrus, lingual gyrus, posterior fusiform gyrus). The largest effect was observed in the middle fusiform gyrus (mFFG, $p = .0106$, $\eta^2 = 0.153$). Thus, we compared CDR values around the N290 peak in the mFFG with a region showing a nonsignificant stimulus effect, namely the aTP ($p = .6098$, $\eta^2 = 0.008$). Fig. 6B displays current density amplitudes in the mFFG (top) and aTP (bottom) separately for faces and objects and across ages. Differences in the CDR values across stimulus type were evident only in the mFFG, with larger values in response to faces than objects. We did not conduct CDR analyses on attention trials for this component, given the null results obtained in the ERP analyses.

An age by stimulus type mixed-ANOVA was performed using CDR values from the mFFG and aTP as multiple dependent variables. The main effect of stimulus type (F (1, 20) = 4.83, $p = .0399$) was better qualified by a significant stimulus type by ROI interaction, F (1, 20) = 12.83, $p = .0019$. To further explore this interaction, we tested the effect of stimulus type on each ROI. Results showed that the CDR values around the peak of the N290 were larger for faces than objects only in the mFFG, F (1, 22) = 13.05, $p = .0015$, $\eta^2 = 0.372$. Fig. 6C shows the maximal CDR values for faces at 12 months in the mFFG (left) and aTP (right), plotted on age-appropriate MRI templates. The level of source activation was high in response to faces across the aTP and mFG, but only the mFG showed a pattern of activation associated with the peak of the N290.

3.4.1. Summary N290

The N290 ERP component showed face specificity. The N290 was larger (i.e., more negative) to faces than objects at parietal and parietal-occipital electrode locations. Additionally, the N290 peak amplitude increased with age. CDR analyses indicated that the N290 originated in the middle fusiform gyrus and surrounding areas. The CDR amplitude of the N290 was not modulated by HR-defined periods of attention or inattention.

3.5. P400 ERP component

Fig. 7A (top panels) shows the P400 ERP responses as a function of time and separately for stimulus type (i.e., faces and objects) at four representative inferior-medial posterior electrodes (i.e., Oz, Iz, PO9, PO10) in 12-month-old infants. On average the P400 component peaks at 465 ms after stimulus onset and shows a larger response to faces than objects over occipital-medial electrodes (e.g., Oz), whereas the opposite pattern of response is evident over occipital-lateral electrodes (e.g., PO9 and PO10). Fig. 8A depicts topographical scalp activity at the P400 peak as a function of faces and objects (top panels). The P400 activity appears to be largest over occipital-lateral electrodes at 12 months of age, and larger for faces than objects across ages. The P400 peak amplitude was analyzed with a stimulus type (faces, objects) by age (4.5, 6, 8, and 12 months) mixed-ANOVA, with medial inferior posterior electrodes as multiple dependent variables. The main effect of age (F (3, 128) = 5.56, $p = .0013$) was qualified by a significant interaction between age and electrode location, F (39, 128) = 2.28, $p < .0001$. To further explore this interaction, we tested the age effect at each electrode location. The results revealed a significant age effect at every electrode location (p's < 0.0001), except for Oz, O2, and Iz (p's > 0.0578), with the largest variance of the model explained at the P7 electrode ($\eta^2 = 0.148$).

We examined the effect of attention on the P400 amplitude. Fig. 7B (top panels) shows the 12-month-olds' P400 ERP responses to faces and objects during attention and inattention as a function of time and separately for some of the electrodes of interest. Similar to the design of previous analyses, the P400 was analyzed as a function of attention type (attention-faces, attention-objects, inattention) and age (4.5, 6, 8, 12 months), using a mixed-ANOVA, with inferior-medial posterior electrodes as multiple dependent variables. The main effects of age (F (3, 125) = 5.74, $p = .0010$) and attention (F (2, 125) = 3.14, $p = .0458$) suggested that P400 amplitude increased with age (4.5 months: $M = 5.52$ μV; 6 months: $M = 9.34$ μV; 8 months: $M = 9.13$ μV; 12 months: $M = 14.47$ μV) and was larger for attention to faces ($M = 10.80$ μV) than attention to objects ($M = 9.75$ μV) and inattention ($M = 8.84$ μV) trials. These effects were qualified by a significant three-way interaction between age, attention and electrode location, F (78, 2223) = 2.06, $p < .0001$. Univariate ANOVAs revealed a significant main effect of electrode location at all ages (p's < 0.0442). Furthermore, at 8 and 12 months we found an interaction between attention and electrode location, for which all the post-hoc comparisons were nonsignificant.

3.6. Sources of P400 ERP component

Preliminary analyses of CDR values around the peak of P400 component showed that there were no significant effects of stimulus type in any of the 16 ROIs. Fig. 8B displays the ERP activity at the peak of P400 (top line) and the respective distribution of current density amplitudes plotted on the age-appropriate MRI templates. The response to faces appears to be localized in the posterior cingulate (PC), with a linear activation increase with age. Line graphs depict current density amplitudes around the peak of P400, separately for faces and objects, in the PC and aTP. Of note, the CDR amplitudes seem to be larger at the aTP than PC, but show peaked patterns only at the PC.

3.6.1. Summary P400

The amplitude of the P400 increased linearly with age, as seen in the N290. Dissimilar to the N290 results, P400 ERP responses were not modulated by stimulus or attention categories. A visual inspection of the distribution of CDR values suggested that the source of the P400 activity could be located around the posterior cingulate. However, none of the ROIs showed differences in the current density amplitudes for faces versus objects.

3.7. Nc ERP component

We analyzed the mean Nc response from 400 to 700 ms after stimulus onset at frontal and central electrode locations (green channels in Fig. 1B). The bottom panels of Fig. 7A show the 12-month-olds' Nc responses to faces and objects as a function of time. The Nc mean amplitude was analyzed in a mixed-ANOVA including stimulus type (faces, objects) and age (4.5, 6, 8, and 12 months) as factors, with multiple electrode locations as dependent variables. The main effect of age (F (3, 128) = 3.84, $p = .0114$) was qualified by a significant three-way interaction between age, stimulus type and electrode location, F (33, 1331) = 2.10, $p = .0003$. We further explored this interaction by performing a univariate ANOVA for each age group. Results revealed a significant main effect of electrode location at all ages (p's < 0.0254). Further, a main effect of stimulus type was found at 4.5 ($p = .0002$), 6 ($p < .0001$), and 8 months ($p < .0001$). The mean amplitude of the Nc was greater for objects than faces at 4.5 months (faces: $M = -2.07$ μV; objects: $M = -2.37$ μV), whereas larger for faces than objects at both 6 (faces: $M = -3.85$ μV; objects: $M = -2.51$ μV) and 8 months of age (faces: $M = -4.79$ μV; objects: $M = -4.01$ μV). The effect of stimulus type at 6 months was qualified by a significant interaction between stimulus type and electrode location ($p < .0001$). Simple effects were further examined through the calculation of the effect sizes, which revealed that the stimulus variance was largely explained at central electrodes (Cz, $\eta^2 = 0.201$; C2, $\eta^2 = 0.193$).

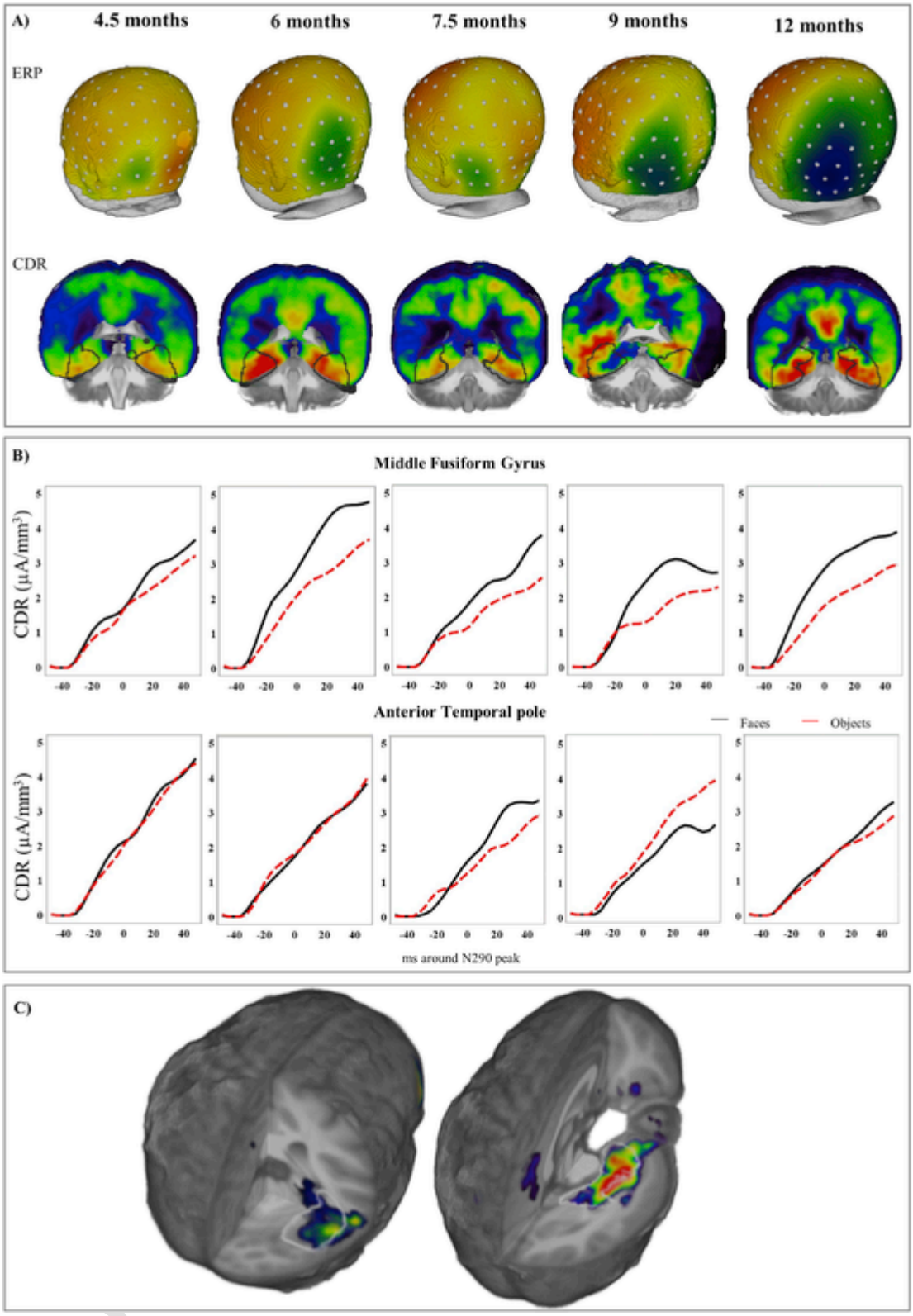

Fig. 6. Panel A shows the N290 ERP and CDR values (coronal view) in response to faces across ages plotted on age-appropriate MRI template. Panel B depicts the line graphs of the CDR values for faces and objects centered at the peak of N290 (from −40 to +40 ms) separately for the testing ages in the middle Fusiform Gyrus and Anterior Temporal pole. Panel C represents the 3D rendering localization of CDR.

Topographical maps in Fig. 9A show the developmental changes in Nc amplitude during attention and inattention over frontal-central electrode locations. Bar charts depict the average Nc response during HR-defined attention in response to faces, objects, and during inattention. Overall, the Nc amplitude increases with age, and the differences in amplitude across attention and inattention trials appear to de-

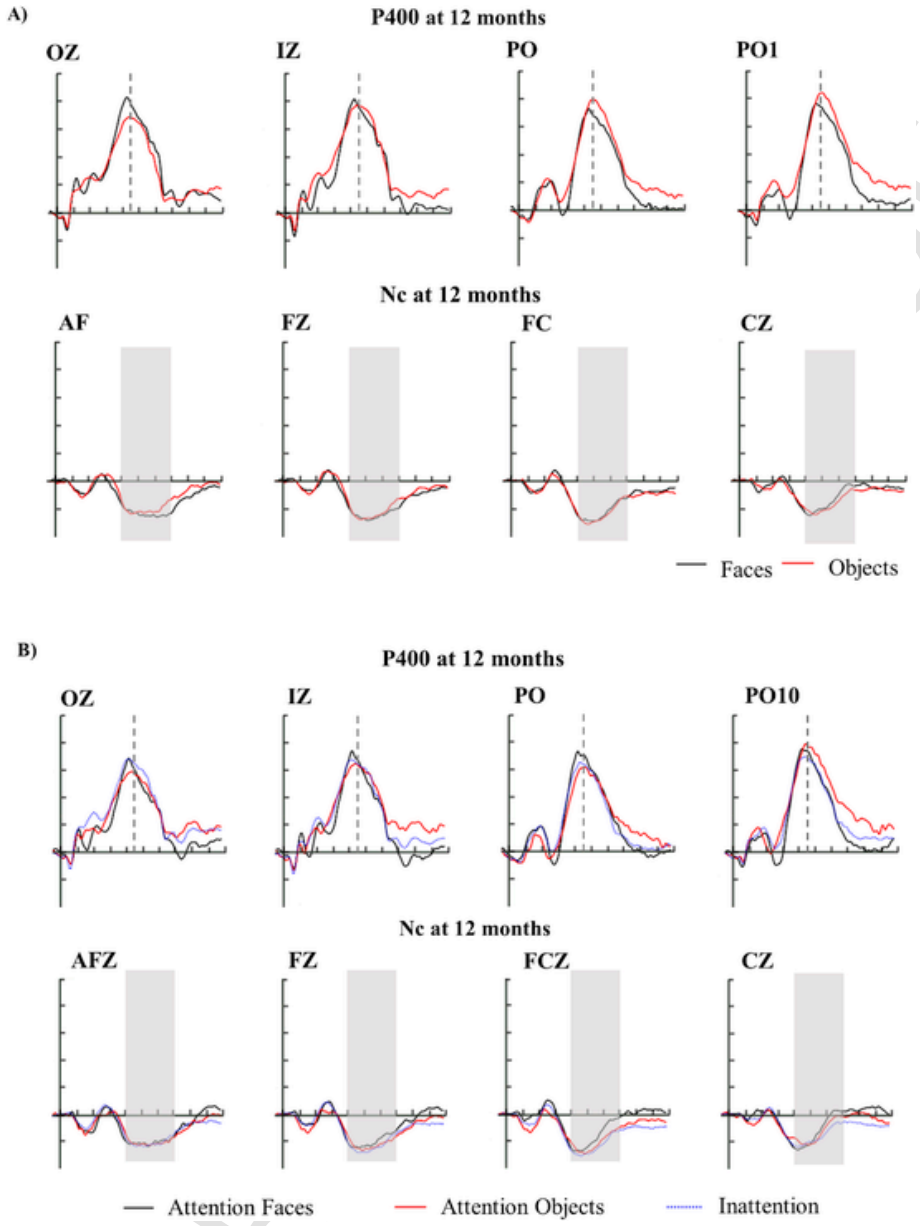

Fig. 7. P400 and Nc ERP grand average (−50 to 1000 ms from stimulus onset) response over a sub-set of inferior-lateral occipital-parietal cannels (P400) and frontal-central channels (Nc). Panel A shows the ERP responses for faces and objects, while panel B depicts P400 and Nc responses for the HR-defined periods of attention to faces, attention to objects and inattention. Amplitudes ±40 ms around the peak of the P400 (dotted vertical lines) and average amplitude within 400–700 ms time window (gray boxes) defined the ERP values for the Nc component. Legend of x-axis and y-axis is reported in Fig. 1B.

crease with age. The Nc mean amplitude was analyzed in an attention type (attention-faces, attention-objects, inattention) by age (4.5, 6, 8, and 12 months) mixed-ANOVA, with multiple frontal-central electrode locations as dependent variables. The main effect of age ($p = .0095$) and the interaction between age and electrode location ($p < .0001$) were qualified by a significant three-way interaction between age, electrode location and attention type, $F(66, 1881) = 1.34$, $p = .0387$. Similar to the previous set of analyses, we further explore the effect of attention type and electrode location with univariate ANOVAs for each age group. The attention effect was significant at 4.5 ($p < .0001$), 6 ($p < .0001$), and 8 months ($p = .0158$), but not at 12 months of age ($p = .1618$). Bonferroni corrected post-hoc comparisons revealed that the Nc amplitude was larger during HR-defined periods of inattention than attention to faces in 4.5-month-old infants ($p = .013$). On the other hand, none of the comparisons reached statistical significance at 8 months ($p > .126$), whereas the effect of attention was better qualified by a significant attention by electrode location interaction at 6 months of age ($p = .0006$). The simple effects, examined through the calculation of the effect sizes, revealed that the attention type variance was largely explained at frontal electrodes (F2, $\eta^2 = 0.207$; Fz, $\eta^2 = 0.203$; F1, $\eta^2 = 0.149$).

3.8. Sources of Nc ERP component

Analyses of the Nc component showed that its amplitude was modulated by the HR-defined periods of attention, thus we explored variations in the current density amplitudes of attention to faces, attention to objects and inattention trials. Preliminary analyses on the 16 ROIs revealed that the attention type effects in the parahippocampal gyrus (PHG, $p = .00043$, $\eta^2 = 0.184$) and lingual gyrus (LG, $p = .0371$, $\eta^2 = 0.205$) explained the highest variance of anterior-lateral and mid-posterior lateral brain areas, respectively. Other ROIs showed a signifi-

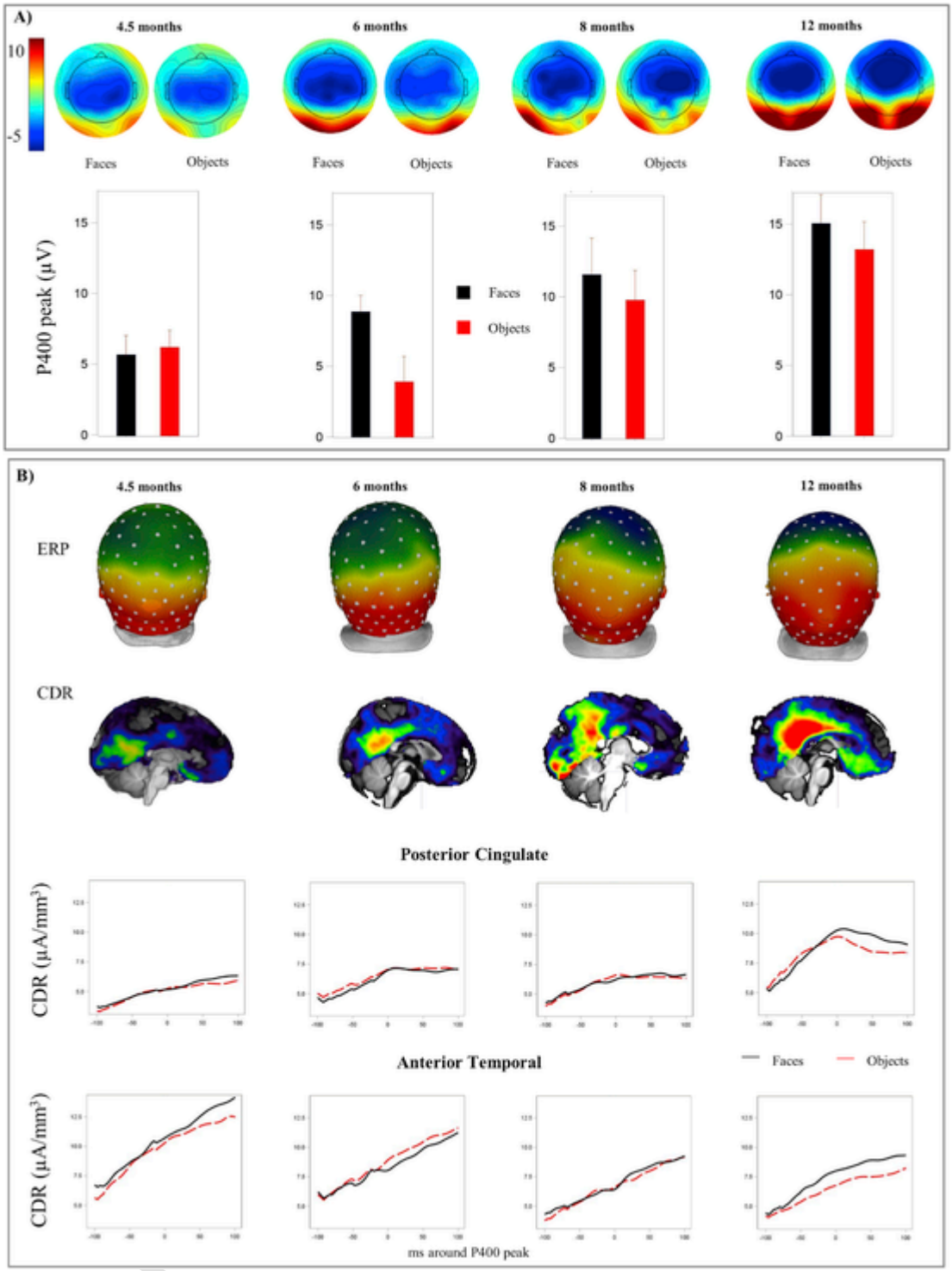

Fig. 8. P400 response to faces and objects across ages. Panel A displays scalp topographical maps at the P400 peak separately for faces and objects (top), and bar graphs of amplitude around the peak of P400 component for faces and objects over all the ages (bottom). Panel B depicts a 3D rendering of ERP and CDR values (sagittal view) at the peak of P400 for faces and objects across ages, and CDR amplitude centered at the peak of P400 (from −40 to +40 ms) separately for the testing ages in the Posterior Cingulate and Anterior Temporal pole.

cant effect of attention (e.g., anterior frontal gyrus, anterior temporal pole, middle fusiform gyrus, inferior temporal gyrus lateral, posterior fusiform gyrus, inferior occipital gyrus lateral). However, these areas explained less variance in the model, thus were not further analyzed. We compared the CDR values within the time-window of the Nc component in the PHG and LG to the current density amplitudes in a region with a nonsignificant attention effect, the orbital-frontal gyrus (orbFG, $p = .1554$, $\eta^2 = 0.180$).

We performed an age by attention type mixed-ANOVA with the CDR values from the selected ROIs as multiple dependent variables. The results showed significant main effects of both attention, F (2, 147) = 26.73, $p < .0001$, and ROI, F (2, 246) = 48.70, $p < .0001$. Bonferroni-corrected contrasts were performed to explore differences between pairs of each attention type and ROI. Line graphs in Fig. 9B (bottom panels) show that CDR values at the PHG were higher and sig-

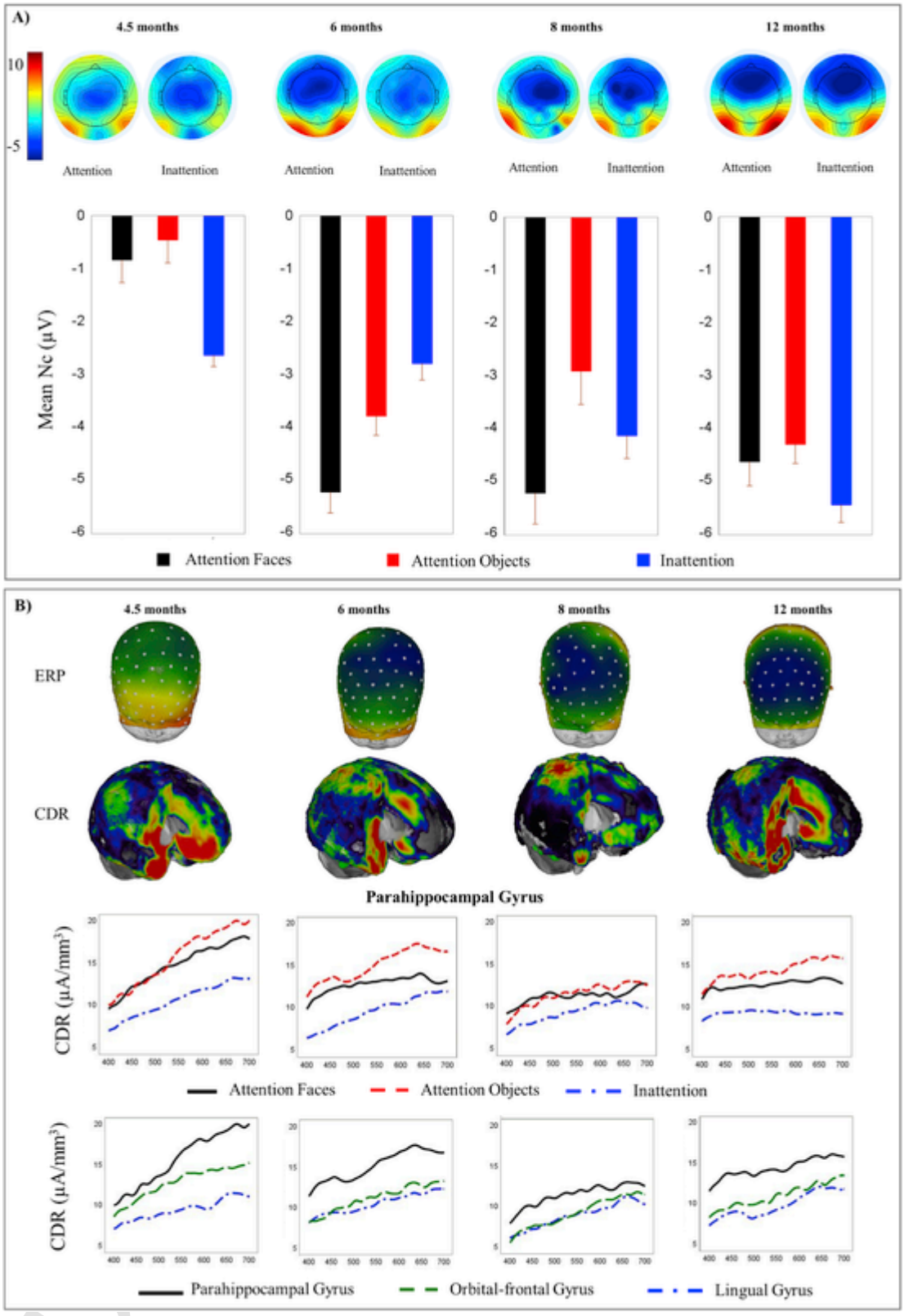

Fig. 9. Nc response the HR-defined periods of attention to faces, attention to objects and inattention across ages. Panel A displays scalp topographical maps at the Nc median latency of each age group separately for periods of attention and inattention (top), and bar graphs of average amplitude of the Nc time window for the three HR-defined categories (bottom). Panel B depicts a 3D rendering of ERP and CDR values (sagittal cut) of the Nc for the HR-defined period of attention to faces, and CDR amplitude during the time window of the Nc component separately for the testing ages in the Orbitofrontal Gyrus and Anterior Temporal pole.

nificantly different than current density amplitudes at the LG and orbFG (p's < 0.0001). Further, the responses to both faces and objects during attention showed greater CDR amplitudes than responses during inattention (p's < 0.0001).

3.8.1. Summary Nc

The mean amplitude of the Nc increased linearly with age in response to both faces and objects across periods of attention and inattention. This age effect was evident over anterior-frontal and frontal electrode locations. Further, the Nc negativity at the frontal electrodes (i.e., F1, FZ, F2) was larger in response to faces during the HR-defined periods of attention than it was in response to objects during attention and to faces and objects during inattention. However, this face specific effect did not emerge in the CDR analyses across any of the considered ROIs. The CDR values of Nc component were largest at the PHG and elicited greater responses during attention than inattention, regardless of the ROI.

4. Discussion

One goal of this study was to explore changes in the morphology of the ERP components in response to face and object stimuli from 4.5 to 12 months of age. The amplitude of the P1 was greater in response to faces than objects, and during attention to faces than attention to objects and inattention trials. The P1 was the only analyzed component that did not show significant changes across ages. The N290 amplitude increased with age and was greater in response to faces than objects at temporal-parietal and temporal-occipital electrodes. The amplitude of the P400 showed a linear increase with increasing age, however its activity was not modulated by either stimulus type or HR-defined attentional phases. The amplitude of the Nc was greater during attention to faces than attention to objects and inattention trials over frontal electrodes only at 6 months, whereas an opposite pattern (i.e. larger Nc amplitude during inattention than attention to face trials) was found at 4.5 months.

Our second goal was to examine the neural sources of those significant effects found in the ERP analyses. The scalp recording at the peak of the P1 component in response to faces and objects was localized primarily in the lingual gyrus, whereas the P1 activity during HR-defined periods of attention to faces was mainly localized in the anterior temporal pole. The source analysis of the N290 component revealed significant levels of activation in the middle fusiform gyrus and other areas adjacent to this ROI, and larger CDR values in response to faces than objects. The examination of the P400 current density values did not reveal significant stimulus effects in any of the considered ROIs. However, qualitative changes in current density, resembling the peak of the P400 ERP component, were visible in the posterior cingulate. Lastly, the source localization of the Nc revealed large activation of the parahippocampal gyrus and greater CDR values during HR-defined periods of attention – to both faces and objects – than inattention.

We were particularly interested in the N290 and its role as a possible precursor of the adult N170. The results indicated that the N290 is a face-sensitive ERP component, evidenced by larger ERP and CDR amplitudes in response to faces than objects across ages that was localized to the middle fusiform gyrus. Scalp topography and distribution of the ERP in response to the visual presentation of faces became progressively more negative with increasing age. Qualitative comparisons of N290 scalp distribution across ages suggest that this component shows a lateralized distribution by 9 months. Both the N290 scalp distribution (Fig. 5A, top panels) and waveform (Fig. 1B, bottom panels) in response to faces, but not objects, were similar at 9 and 12 months. It has extensively reported that, around 9 months, infants begin to exhibit face-processing biases (Maurer and Werker, 2014), and expert discrimination and recognition abilities for the most experienced category of faces (Scherf and Scott, 2012). This evidence, along with the structural brain modifications (e.g., myelination, Uda et al., 2015; Richards and Conte, 2019 and Conte and Richards, 2019) and the changes in the neural responses to faces (for a review, see Hoehl and Peykarjou, 2012), suggests that by the end of the first year of life the N290 likely represents the electrophysiological marker of face-processing in infants.

Past ERP research on face-processing in infants has focused on different subsets of electrode clusters (medial electrode sites: Kouider et al., 2013; Peykarjou et al., 2014; Scott and Monesson, 2010; lateral sites: Key and Stone, 2012; Macchi Cassia et al., 2006; McCleery et al., 2009; medial and lateral sites: de Haan et al., 2002; Halit et al., 2004; Halit et al., 2003; Leppanen et al., 2007). As a consequence, a limited comparison of the N290 ERP findings in the literature can be done. We used spherical spline interpolation of the data from the EGI-126 channels into the 81 channels of the 10-10 system. This interpolation maximized the use of the information in the original channels and allowed us to translate the electrode locations into the 10-10 coordinate system in order to describe our results using a standard system for electrode placement. The N290 responses in this study were distributed over lateral inferior temporal-parietal and temporal-occipital electrodes (i.e., P7 to P10, PO7 to PO10). This might be expected since the source of the N290 was localized in the fusiform gyrus and the projections from the fusiform gyrus to the scalp were in the inferior temporal-occipital electrodes. Therefore, an optimal N290 measurement should take into account these scalp areas with an electrode coverage extending below the traditional 10–20 layout. Further, an exploration of the individual scalp distribution of the ERP activity at the peak of the N290 suggested important differences between participants. Fig. 5B shows these differences by plotting the scalp pattern of the N290 peak for faces of the 12-months age-group on an average template, and four participants on either a self or close MRI template. Such large individual differences in the distribution of the N290 activity have been shown in the activity of the adult N170 (Gao et al., 2019). Thus, it is critical for a comprehensive investigation of infants' neural responses to faces to consider the electrical activity recorded at inferior scalp areas.

The areas of significant activation at the N290 peak were in the posterior ventral temporal lobe and showed a similar localization found in previous infant studies exploring the cortical sources of the response to face-like patterns in newborns (Buiatti et al., 2019), as well as the source of the N290 in response to faces (Guy et al., 2016; Johnson et al., 2005). Specifically, the analysis of cortical sources of the N290 component revealed significant levels of activation in the middle fusiform gyrus and neighboring areas (e.g., the posterior fusiform gyrus). Current density response occurring in the middle fusiform gyrus showed a peaked response (Fig. 6B), and significantly larger activity in response to faces than objects. This peaked activity was especially marked in the 9- and 12-month-olds' response to face stimuli and coincided with the N290 deflection in the ERP data. Areas within the fusiform gyrus have been implicated in face processing in adult studies of source analysis of the N170 (Deffke et al., 2007; Gao et al., 2019; Rossion et al., 2003; Shibata et al., 2002) and as the site of the fMRI-defined fusiform face area in adults (Kanwisher et al., 1997). Recent metanalyses of fMRI studies support the role of the right middle FG and posterior FG across a large number of stimuli and tasks (Berman et al., 2010; Müller et al., 2018). Only one fMRI study has investigated the processing of faces infants. Results from this study suggests that infants at 4–6 months of age have an adult-like functional organization of responses to faces (Deen et al., 2017).

These results are consistent with three studies investigating the generators of the ERP responses to faces in infants. One study utilized data collected in prior studies of infants viewing different face orientations and direct and averted gaze to localize the source of the N290 ERP response (Johnson et al., 2005). The primary aim of this study was

to determine whether brain areas active during the processing of faces in adults characterized the face-processing network in infants as well. An equivalent current dipole analysis was completed and identified dipoles in the fusiform gyrus, right STS and surrounding temporal lobe areas, lateral occipital cortex, and certain prefrontal regions. Three-, 4-, and 12-month-olds were tested and all the identified brain regions were active during the processing of faces. These regions discriminated upright to inverted faces around the latency of the N290 in 3- and 12-month-old infants, suggesting that similar regions involved in adult face-processing network were active in infancy (Johnson et al., 2005). Similarly, Guy et al. (2016) examined developmental changes in and cortical sources of the N290 in response to familiar and unfamiliar faces and toys in infants at 4.5, 6, and 7.5 months of age. The cortical source of the N290 was localized in the middle fusiform gyrus, anterior fusiform gyrus, parahippocampal gyrus, and temporal pole. These brain regions showed an increasing activation in response to faces and toys with age (Guy et al., 2016). The results of a recent study identified the fusiform and inferior occipital gyri as generators of the N290 during the discrimination of emotional valence of faces in 5- and 7-month-old infants (Xie et al., 2019). In line with these studies, our findings indicate that several occipito-temporal areas, including the posterior fusiform gyrus, showed large CDR values in response to visual stimuli at the peak of the N290 ERP component. However, the sources of the N290 in the middle fusiform gyrus showed the greatest difference between faces and objects and had the same peaked amplitude at the peak of the N290, suggesting the development of face categorization responses in this brain area.

We also explored the activity of the P1, P400 and Nc ERP components. The results of the P1 showed larger amplitude in response to faces than objects at medial inferior posterior electrodes with the largest effect obtained at the Oz channel. Current density reconstruction analyses revealed that the P1 activity originated in the lingual gyrus. Few studies have previously considered changes of the P1 activity in response to faces in infancy, since the responses reported on the level of the P1 in adults (Herrmann et al., 2005) have been attributed to differences in low-level characteristics (e.g. amplitude spectrum, color) of the stimuli (Rossion and Caharel, 2011). Our study was not designed to assess this hypothesis, thus the difference between faces and objects in the P1 amplitude could reflect the differences in shape or other low-level features of our stimuli. Further studies should control for low-level properties using ideally matched control stimuli, such as phase-scrambled stimuli (e.g. Rossion and Caharel, 2011), stimuli of similar complexity, and stimuli matched for size.

Two noteworthy observations came from our results on the P1 ERP component. First, the P1 was the only ERP response that did not change in amplitude with increasing age. Although the topographical distribution on the scalp (Fig. 4A) seems to suggest a slight increase of the response at the peak of P1, this change did not reach statistical significance. Second, infants' attentional states exerted an influence on the P1 amplitude across ages. That is, we observed larger responses to faces during HR-defined attention than to objects during attention and to faces and objects during inattention. This effect was mainly localized to the anterior temporal pole. The attentional modulation of the P1 response may be due to differences in low-level characteristics of our stimuli, similar to the proposed differences in the comparison of faces and objects. Overall, we cannot conclude that the P1 is a face-sensitive ERP component in infancy. However, the specific amplitude changes in response to faces modulated by infant's attentional status leave open the possibility of an influence of top-down factors on early stages of face processing. The extent to which the P1 is a face-specific ERP component in infancy should be investigated in future research employing stimuli matched in low-level visual characteristics.

The results of the analysis of the P400 found that this component increased with age, did not differentiate face and object stimuli, and was not modulated by the HR-defined periods of attention. Previous studies of the role of face processing in infants have reported inconsistent results for the P400. The majority of these studies showed no face sensitivity on the P400 amplitude response (Balas et al., 2011; Conte et al., 2019; Guy et al., 2018; Halit et al., 2004; Macchi Cassia et al., 2006; Peykarjou and Hoehl, 2013; Xie and Richards, 2016). Conversely, other studies suggested that the P400 amplitude is sensitive to the face orientation (de Haan et al., 2002; Halit et al., 2003), stimulus familiarity (Key et al., 2009; Scott et al., 2006), attentional status (Guy et al., 2016) and emotional face-processing (Xie et al., 2019). A variety of results have been observed in comparison of faces and objects, including larger amplitude responses to toys than faces (McCleery et al., 2009; Guy et al., 2016), shorter peak latency to faces than toys (de Haan and Nelson, 1999), and no modulation of stimulus type (Guy et al., 2018; Peykarjou and Hoehl, 2013; Xie et al., 2019). The results of the CDR analysis in the current study did not find discrimination of faces and objects. The likely source of the P400 was the posterior cingulate, but activity in this ROI did not distinguish faces and objects. Our results do not support the hypothesis of the P400 as a face-specific component involved in categorization processes.

Lastly, we investigated whether previous findings on the Nc amplitude can be extended to the processing of faces. We examined potential differences in the Nc amplitude during HR-defined periods of attention to faces, attention to objects and inattention, because the Nc activity has been reported as a marker of the attention allocation and arousal in infants (Reynolds et al., 2010; Reynolds and Richards, 2005, 2009; Richards, 2003). Previous research has revealed that the Nc amplitude increases during periods of attention when compared to inattention, regardless of stimulus type (i.e., computer-generated geometric patterns, Reynolds and Richards, 2005; faces and toys, Guy et al., 2016). Further, the Nc amplitude has been reported to discriminate familiar and unfamiliar faces (Guy et al., 2018; de Haan and Nelson, 1999) and emotional faces (Leppanen et al., 2007; Nelson and de Haan, 1996; Quadrelli et al., 2019; Xie et al., 2019). In line with these findings, our results indicated that the Nc activity was modulated by both stimulus type and infants' attentional state. Interestingly, different effects qualified the Nc responses at different ages: at 4.5 months, participants showed larger Nc amplitude in response to objects than faces, and during inattention than attention to face trials, whereas in older participants the Nc amplitude was larger for faces than objects (i.e., at 6 and 8 months of age), and for attention to face than attention to object and inattention trials (i.e., 6 months). Nonsignificant Nc differences were found in 12-month-old infants.

Previous studies comparing Nc responses to faces and non-faces have found that this component is modulated primarily by attention and stimulus familiarity (e.g., familiar faces and toys; de Haan and Nelson, 1999; Guy et al., 2016, 2018). Further, larger Nc amplitude has been reported in response to faces than toys in young infants (up to 7.5 months of age; Xie et al., 2019), whereas larger amplitude seemed to characterize the Nc response to objects than faces in 10-month-old infants (McCleery et al., 2009). The results of our study showed that there were some age differences in the extent to which the Nc activity was modulated by both stimulus type and attention. Specifically, the Nc amplitude in 4.5-month-old participants was larger in amplitude in response to objects than faces and larger during HR-defined periods of inattention in response to faces and objects than periods of attention in response to faces. On the other hand, an opposite pattern was found in 6- and 8-month-old infants, the Nc was greater in response to faces than objects. Only at 6 months of age were HR-defined phases of attention associated with increased amplitude in response to faces. Overall, it seems that stimulus type and attention modulate the Nc response in young participants, whereas these effects are leveled out later in the first year of life.

The CDR values within the time-window of the Nc component were larger during periods of attention, to both face and object stimuli, than inattention trials across ages. We found larger CDR activity in the parahippocampal gyrus than posterior and anterior regions (i.e., lingual and orbital-frontal gyri), although the effect of infant's attentional state was not localized in a single brain area. Only two studies have previously investigated the source localization of the Nc activity to faces in infants, and both have considered the average activity of the ERP in the time windows of the P400 and Nc (Guy et al., 2016; Xie et al., 2018). Guy et al. (2016) found that P400/Nc ERP amplitude was greater during periods of attention in response to faces than objects in the middle fusiform and middle inferior temporal gyri at 4.5 months of age. A second study localized the P400/Nc in response to emotional faces to the posterior cingulate cortex/precuneus at 5 and 7 months of age, and reported greater activation in response to angry than happy and fearful faces across ages (i.e., 5, 7, and 12 months; Xie et al., 2019).

Our results imply that the P400 and Nc are separate ERP components. The posterior-positive/anterior-negative scalp distribution is similar for these two components and this and their overlapping time windows could lead to the conclusion of a single ERP component with a single dipole source. However, their timing, shape, and cortical sources implies two ERP components influenced by separate cognitive processes. The P400 had a peaked response at about 465 ms following stimulus onset, whereas the Nc shows a gradual response from about 350 to 750 ms (Fig. 7). Our results show distinct source areas for the P400 (posterior cingulate, Fig. 8B) and Nc (anterior areas, parahippocampal gyrus, Fig. 9B). Finally, the functional relations in this and other studies suggests that the Nc indexes cognitive processes that involve attention to novel or interesting stimuli. A recent review emphasized some commonalities between the functional characteristics and source localization of the infant Nc and the adult P300. Both these components seem to originate in anterior brain areas and index attentional processes and stimulus probability in familiarization/learning procedures (Riggins and Scott, 2019). Our results are in line with this view and provide a further evidence of the role of the Nc in the allocation of attentional resources.

The results of the current study revealed developmental changes in face-sensitive ERP responses and their neural sources across the first year of life. Further, our findings indicate that attention plays a role in differentiating responses to faces and objects. This study systematically compared infants' neural responses to faces and objects and localized the sources of face-sensitive ERP activity in the first year of life. Enhanced amplitude responses to face stimuli were recorded in both the P1 and N290 ERP components, which was localized to the lingual and middle fusiform gyri, respectively. Despite evidence of face-sensitivity of the P1, further research matching low-level visual characteristics of face and non-face is necessary to reach this conclusion. Amplitude of the P400 did not differentiate responses to faces and objects and was not modulated by infants' attentional phase, suggesting that P400 responses are not broadly associated with face processing. Further investigation of the P400 response to other stimulus aspects, such as the orientation, is necessary to fully understand the role of this component in infant face-processing. Finally, results of the Nc analysis indicate that its level of activation may distinguish the encoding of faces and objects, especially at younger ages, and relate to infant's attentional state. Taken together, the current findings provide a better understanding of the development of face-sensitive ERP responses and their neural sources in the first year of life.

Notes

[1] Demographic information of 7.5- and 9-month-old participants are reported in Supplementary Table 1. Statistical analyses considering participants at these ages as separate groups are reported in Supplementary Material 1.

2 The current analyses used data from the Xie and Richards study from the medium and long ISIs (600–1000 ms, and 1500–2000 ms) and excluded the short ISI trials (400–600 ms) in order to have trials of comparable ISIs as the Guy et al., Richards, and Conte and Richards studies.

Acknowledgment

This research was supported by a grant from the National Institute of Child Health and Human Development (NICHD-R01-HD18942) to J. E. Richards and from the National Institute of Mental Health (NIMH R01-MH090194) to J. E. Roberts.

Appendix A. Supplementary data

Supplementary data to this article can be found online at https://doi.org/10.1016/j.neuroimage.2020.116602.

Uncited references

Itier and Taylor, 2004a,b, Richards and Conte,.

References

Ackles, P.K., Cook, K.G., 2007. Attention or memory? Effects of familiarity and novelty on the Nc component of event-related brain potentials in six-month-old infants. Int. J. Neurosci. 117 (6), 837–867. doi:10.1080/00207450600909970.

Ackles, P.K., Cook, K.G., 2009. Event-related brain potentials and visual attention in six-month-old infants. Int. J. Neurosci. 119 (9), 1446–1468. doi:10.1080/00207450802330579.

Balas, B., Westerlund, A., Hung, K., Nelson, C.A., 2011. Shape, color and the other-race effect in the infant brain. Dev. Sci. 14 (4), 892–900. doi:10.1111/j.1467-7687.2011.01039.x.

Bentin, S., Allison, T., Puce, A., Perez, E., McCarthy, G., 1996. Electrophysiological studies of face perception in humans. J. Cognit. Neurosci. 8 (6), 551–565. doi:10.1162/jocn.1996.8.6.551.

Berman, M.G., Park, J., Gonzalez, R., Polk, T.A., Gehrke, A., Knaffla, S., Jonides, J., 2010. Evaluating functional localizers: the case of the FFA. Neuroimage 50 (1), 56–71. doi:10.1016/j.neuroimage.2009.12.024.

Bernstein, M., Yovel, G., 2015. Two neural pathways of face processing: a critical evaluation of current models. Neurosci. Biobehav. Rev. 55, 536–546. doi:10.1016/j.neubiorev.2015.06.010.

Buiatti, M., Di Giorgio, E., Piazza, M., Polloni, C., Menna, G., Taddei, F., Baldo, E., Vallortigara, G., 2019. Cortical route for facelike pattern processing in human newborns. Proc. Natl. Acad. Sci. Unit. States Am. 116 (10), 4625–4630. doi:10.1073/pnas.1812419116.

Caldara, R., Thut, G., Servoir, P., Michel, C.M., Bovet, P., Renault, B., 2003. Face versus non-face object perception and the 'other-race' effect: a spatio-temporal event-related potential study. Clin. Neurophysiol. 114 (3), 515–528. doi:10.1016/s1388-2457(02)00407-8.

Carmel, D., Bentin, S., 2002. Domain specificity versus expertise: factors influencing distinct processing of faces. Cognition 83, 29.

Carver, L.J., Dawson, G., Panagiotides, H., Meltzoff, A.N., McPartland, J., Gray, J., Munson, J., 2003. Age-related differences in neural correlates of face recognition during the toddler and preschool years. Dev. Psychobiol. 42 (2), 148–159. doi:10.1002/dev.10078.

Conte, S., Proietti, V., Quadrelli, E., Turati, C., Cassia, V.M., 2019. Sibling experience prevents neural tuning to adult faces in 10-month-old infants. Neuropsychologia 129, 72–82. doi:10.1016/j.neuropsychologia.2019.03.010.

Conte, S., Richards, J.E., 2019. The Development of Face Sensitive Cortical Processing in Early Infancy. Paper presented at the Society for Research in Child Development, Baltimore, MD.

Courchesne, E., Ganz, L., Norcia, A.M., 1981. Event-related brain potentials to human faces in infants. Child Dev. 52 (3), 804–811.

de Haan, M., Belsky, J., Reid, V., Volein, A., Johnson, M.H., 2004. Maternal personality and infants' neural and visual responsivity to facial expressions of emotion. JCPP (J. Child Psychol. Psychiatry) 45 (7), 1209–1218. doi:10.1111/j.1469-7610.2004.00320.x.

de Haan, M., Johnson, M.H., Halit, H., 2003. Development of face-sensitive event-related potentials during infancy: a review. Int. J. Psychophysiol. 51 (1), 45–58. doi:10.1016/s0167-8760(03)00152-1.

de Haan, M., Johnson, M.H., Halit, H., 2007. Development of face-sensitive ERPs. In: de Haan, M. (Ed.), Infant EEG and Event-Related Potentials. Psychology Press, New York, pp. 77–99.

de Haan, M., Nelson, C.A., 1997. Recognition of the mother's face by six-month-old infants: a neurobehavioral study. Child Dev. 68 (2), 187–210.

de Haan, M., Nelson, C.A., 1999. Brain activity differentiates face and object processing in 6-month-old infants. Dev. Psychol. 35 (4), 1113–1121.

de Haan, M., Pascalis, O., Johnson, M.H., 2002. Specialization of neural mechanisms underlying face recognition in human infants. J. Cognit. Neurosci. 14 (2), 199–209.

Deen, B., Richardson, H., Dilks, D.D., Takahashi, A., Keil, B., Wald, L.L., et al., 2017. Organization of high-level visual cortex in human infants. Nat. Commun. 8, 13995.
Deffke, I., Sander, T., Heidenreich, J., Sommer, W., Curio, G., Trahms, L., Lueschow, A., 2007. MEG/EEG sources of the 170-ms response to faces are co-localized in the fusiform gyrus. Neuroimage 35 (4), 1495–1501. doi:10.1016/j.neuroimage.2007.01.034.
Delorme, A., Makeig, S., 2004. EEGLAB: an open source toolbox for analysis of single-trial EEG dynamics including independent component analysis. J. Neurosci. Methods 134 (1), 9–21. doi:10.1016/j.jneumeth.2003.10.009.
Dennis, T.A., Malone, M.M., Chen, C.-C., 2009. Emotional face processing and emotion regulation in children: an ERP study. Dev. Neuropsychol. 34 (1), 85–102. doi:10.1080/87565640802564887.
Di Russo, F., Martinez, A., Sereno, M.I., Pitzalis, S., Hillyard, S.A., 2002. Cortical sources of the early components of the visual evoked potential. Hum. Brain Mapp. 15 (2), 95–111. doi:10.1002/Hbm.10010.
Eimer, M., 2000. Effects of face inversion on the structural encoding and recognition of faces: evidence from event-related potentials. Cognit. Brain Res. 10, 145–158.
Eimer, M., 2000. Event-related brain potentials distinguish processing stages involved in face perception and recognition. Clin. Neurophysiol. 111, 694–705.
Farroni, T., Csibra, G., Simion, F., Johnson, M.H., 2002. Eye contact detection in humans from birth. Proc. Natl. Acad. Sci. U.S.A. 99 (14), 9602–9605. doi:10.1073/pnas.152159999.
Fillmore, P., Richards, J.E., Phillips-Meek, M.C., Connington, A., Stevens, M., 2014. Stereotaxic MRI Brain Atlases for Infants from 3 to 12 Months.
Gao, C., Conte, S., Richards, J.E., Xie, W., Hanayik, T., 2019. The neural sources of N170: understanding timing of activation in face-selective areas. Psychophysiology 56 (6), e13336. doi:10.1111/psyp.13336.
Grossmann, T., Striano, T., Friederici, A.D., 2006. Crossmodal integration of emotional information from face and voice in the infant brain. Dev. Sci. 9 (3), 309–315.
Guy, M.W., Reynolds, G.D., Zhang, D., 2013. Visual attention to global and local stimulus properties in 6-month-old infants: individual differences and event-related potentials. Child Dev. 84 (4), 1392–1406. doi:10.1111/cdev.12053.
Guy, M.W., Richards, J.E., Tonnsen, B.L., Roberts, J.E., 2018. Neural correlates of face processing in etiologically-distinct 12-month-old infants at high-risk of autism spectrum disorder. Dev. Cogn. Neurosci. doi:10.1016/j.dcn.2017.03.002.
Guy, M.W., Zieber, N., Richards, J.E., 2016. The cortical development of specialized face processing in infancy. Child Dev. doi:10.1111/cdev.12543.
Halit, H., Csibra, G., Volein, A., Johnson, M.H., 2004. Face-sensitive cortical processing in early infancy. JCPP (J. Child Psychol. Psychiatry) 45 (7), 1228–1234. doi:10.1111/j.1469-7610.2004.00321.x.
Halit, H., de Haan, M., Johnson, M.H., 2003. Cortical specialisation for face processing: face-sensitive event-related potential components in 3- and 12-month-old infants. Neuroimage 19 (3), 1180–1193. doi:10.1016/s1053-8119(03)00076-4.
Herrmann, M.J., Ehlis, A.C., Muehlberger, A., Fallgatter, A.J., 2005. Source localization of early stages of face processing. Brain Topogr. 18 (2), 77–85. doi:10.1007/s10548-005-0277-7.
Hoehl, S., Peykarjou, S., 2012. The early development of face processing--what makes faces special? Neurosci. Bull. 28 (6), 765–788. doi:10.1007/s12264-012-1280-0.
Itier, R.J., Latinus, M., Taylor, M.J., 2006. Face, eye and object early processing: what is the face specificity? Neuroimage 29 (2), 667–676. doi:10.1016/j.neuroimage.2005.07.041.
Itier, R.J., Taylor, M.J., 2004a. Face recognition memory and configural processing: a developmental ERP study using upright, inverted, and contrast-reversed faces. J. Cognit. Neurosci. 16 (3), 487–502.
Itier, R.J., Taylor, M.J., 2004b. Source analysis of the N170 to faces and objects. Neuroreport 15 (8), 1261–1265.
Johnson, M.H., de Haan, M., Oliver, A., Smith, W., Hatzakis, H., Tucker, L.A., Csibra, G., 2001. Recording and analyzing high-density event-related potentials with infants using the Geodesic sensor net. Dev. Neuropsychol. 19 (3), 295–323. doi:10.1207/S15326942dn1903_4.
Johnson, M.H., Griffin, R., Csibra, G., Halit, H., Farroni, T., de Haan, M., et al., 2005. The emergence of the social brain network: evidence from typical and atypical development. Dev. Psychopathol. 17 (3), 599–619. doi:10.1017/S0954579405050297.
Kanwisher, N., McDermott, J., Chun, M.M., 1997. The fusiform face area: a module in human extrastriate cortex specialized for face perception. J. Neurosci. 17 (11), 4302–4311.
Karrer, J.H., Karrer, R., Bloom, D., Chaney, L., Davis, R., 1998. Event-related brain potentials during an extended visual recognition memory task depict delayed development of cerebral inhibitory processes among 6-month-old infants with Down syndrome. Int. J. Psychophysiol. 29 (2), 167–200.
Key, A.P., Stone, W., Williams, S.M., 2009. What do infants see in faces? ERP evidence of different roles of eyes and mouth for face perception in 9-month-old infants. Infant Child Dev. 18 (2), 149–162. doi:10.1002/icd.600.
Key, A.P., Stone, W.L., 2012. Processing of novel and familiar faces in infants at average and high risk for autism. Dev. Cogn. Neurosci. 2 (2), 244–255. doi:10.1016/j.dcn.2011.12.003.
Kouider, S., Stahlhut, C., Gelskov, S.V., Barbosa, L.S., Dutat, M., de Gardelle, V., et al., 2013. A neural marker of perceptual consciousness in infants. Science.
Kuefner, D., de Heering, A., Jacques, C., Palmero-Soler, E., Rossion, B., 2010. Early visually evoked electrophysiological responses over the human brain (P1, N170) show stable patterns of face-sensitivity from 4 years to adulthood. Front. Hum. Neurosci. 3, 67. doi:10.3389/neuro.09.067.2009.
Leppanen, J.M., Moulson, M.C., Vogel-Farley, V., Nelson, C.A., 2007. An ERP study of emotional face processing in the adult and infant brain. Child Dev. 78 (1), 232–245.
Lopez-Calderon, J., Luck, S.J., 2014. ERPLAB: an open-source toolbox for the analysis of event related potentials. Front. Hum. Neurosci. 8. doi:Artn 213. Doi: 0.3389/Fnhum.2014.00213.
Luyster, R.J., Powell, C., Tager-Flusberg, H., Nelson, C.A., 2014. Neural measures of social attention across the first years of life: characterizing typical development and markers of autism risk. Dev. Cogn. Neurosci. 8, 131–143. doi:10.1016/j.dcn.2013.09.006.
Luyster, R.J., Wagner, J.B., Vogel-Farley, V., Tager-Flusberg, H., Nelson, C.A., 3rd, 2011. Neural correlates of familiar and unfamiliar face processing in infants at risk for autism spectrum disorders. Brain Topogr. 24 (3–4), 220–228. doi:10.1007/s10548-011-0176-z.
Macchi Cassia, V., Kuefner, D., Westerlund, A., Nelson, C.A., 2006. A behavioural and ERP investigation of 3-month-olds' face preferences. Neuropsychologia 44 (11), 2113–2125. doi:10.1016/j.neuropsychologia.2005.11.014.
Mallin, B.M., Richards, J.E., 2012. Peripheral stimulus localization by infants of moving stimuli on complex backgrounds. Infancy 17 (6), 692–714. doi:10.1111/j.1532-7078.2011.00109.x.
Martinos, M., Matheson, A., de Haan, M., 2012. Links between infant temperament and neurophysiological measures of attention to happy and fearful faces. JCPP (J. Child Psychol. Psychiatry) 53 (11), 1118–1127. doi:10.1111/j.1469-7610.2012.02599.x.
Maurer, D., Werker, J.F., 2014. Perceptual narrowing during infancy: a comparison of language and faces. Dev. Psychobiol. 56 (2), 154–178. doi:10.1002/dev.21177.
McCleery, J.P., Akshoomoff, N., Dobkins, K.R., Carver, L.J., 2009. Atypical face versus object processing and hemispheric asymmetries in 10-month-old infants at risk for autism. Biol. Psychiatr. 66 (10), 950–957. doi:10.1016/j.biopsych.2009.07.031.
Müller, V.I., Höhner, Y., Eickhoff, S.B., 2018. Influence of task instructions and stimuli on the neural network of face processing: an ALE meta-analysis. Cortex 103, 240–255. doi:10.1016/j.cortex.2018.03.011.
Nelson, C.A., 1994. Neural Correlates of Recognition Memory in the First Postnatal Year Human Behavior and the Developing Brain. The Guilford Press, New York, NY, US, pp. 269–313.
Nelson, C.A., Collins, P.F., 1991. Event-related potential and looking-time analysis of infants' responses to familiar and novel events: implications for visual recognition memory. Dev. Psychol. 27 (1), 50–58.
Nelson, C.A., Collins, P.F., 1992. Neural and behavioral correlates of visual recognition memory in 4- and 8-month-old infants. Brain Cognit. 19, 105–121.
Nelson, C.A., de Haan, M., 1996. Neural correlates of infants' visual responsiveness to facial expressions of emotion. Dev. Psychobiol. 29 (7), 577–595.
Oostenveld, R., Fries, P., Maris, E., Schoffelen, J.M., 2011. FieldTrip: Open source software for advanced analysis of MEG,EEG, and invasive electrophysiological data. Computational Intelligence and Neuroscience doi:https://doi. org/10.1155/2011/156869.
Parise, E., Handl, A., Striano, T., 2010. Processing faces in dyadic and triadic contexts. Neuropsychologia 48 (2), 518–528. doi:10.1016/j.neuropsychologia.2009.10.012.
Pascual-Marqui, R.D., 2007. Discrete, 3D distributed, linear imaging methods of electric neuronal activity. Part 1: exact, zero error localization. Signal Process. 81, 855–870. http://arxiv.org/pdf/0710.3341.
R.D. Pascual-Marqui D. Lehmann M. Koukkou K. Kochi P. Anderer B. Saletu ... T. Kinoshita Assessing interactions in the brain with exact low-resolution electromagnetic tomographyPhil. Trans. Math. Phys. Eng. Sci.36919522011 3768378410.1098/rsta.2011.0081
Pempek, T.A., Kirkorian, H.L., Richards, J.E., Anderson, D.R., Lund, A.F., Stevens, M., 2010. Video comprehensibility and attention in very young children. Dev. Psychol. 46 (5), 1283–1293. doi:10.1037/a0020614.
Peykarjou, S., Hoehl, S., 2013. Three-month-olds' brain responses to upright and inverted faces and cars. Dev. Neuropsychol. 38 (4), 272–280. doi:10.1080/87565641.2013.786719.
Peykarjou, S., Pauen, S., Hoehl, S., 2014. How do 9-month-old infants categorize human and ape faces? A rapid repetition ERP study. Psychophysiology 51 (9), 866–878. doi:10.1111/psyp.12238.
Peykarjou, S., Westerlund, A., Cassia, V.M., Kuefner, D., Nelson, C.A., 2013. The neural correlates of processing newborn and adult faces in 3-year-old children. Dev. Sci. 16 (6), 905–914. doi:10.1111/desc.12063.
Phillips, M.C., Richards, J.E., Stevens, M., Connington, A., 2013. A Stereotaxic MRI Brain Atlas for Infant Participants. Paper presented at the Society for Research in Child Development, Seattle, WA.
Quadrelli, E., Conte, S., Macchi Cassia, V., Turati, C., 2019. Emotion in motion: facial dynamics affect infants' neural processing of emotions. Dev. Psychobiol. 1–16. 00. doi:10.1002/dev.21860.
Regan, D., 1989. Human Brain Electrophysiology: Evoked Potentials and Evoked Magnetic Fields in Science and Medicine. Elsevier, New York.
Reynolds, G.D., Courage, M.L., Richards, J.E., 2010. Infant attention and visual preferences: converging evidence from behavior, event-related potentials, and cortical source localization. Dev. Psychol. 46 (4), 886–904. doi:10.1037/a0019670.
Reynolds, G.D., Richards, J.E., 2005. Familiarization, attention, and recognition memory in infancy: an event-related potential and cortical source localization study. Dev. Psychol. 41 (4), 598–615. doi:10.1037/0012-1649.41.4.598.
Reynolds, G., Richards, J.E., 2007. A Developmental Psychophysiological Perspective. Dev. Psychophysiol.: Theory, Syst. Methods 173.
Reynolds, G.D., Richards, J.E., 2009. Cortical source localization of infant cognition. Dev. Neuropsychol. 34 (3), 312–329. doi:10.1080/87565640902801890.
Richards, J.E., 2001. Attention in young infants: a developmental psychophysiological perspective. Handbook Dev. Cognit. Neurosci. 2, 479–497.
Richards, J.E., 2003. Attention affects the recognition of briefly presented visual stimuli in infants: an ERP study. Dev. Sci. 6 (3), 312–328. doi:10.1111/1467-7687.00287.
Richards, J.E., 2013. Cortical sources of ERP in prosaccade and antisaccade eye movements using realistic source models.. Frontiers in Systems Neuroscience 7 (27), 1–20. doi:https://doi.org/10.3389/fnsys.2013.00027.
Richards, J.E., 2015. Brain Responses of 9-Month-Old Infants to Faces and Toys. Department of Psychology, University of South Carolina. Unpublished manuscript.
Richards, J.E., Casey, B.J., 1992. Development of Sustained Visual Attention in the Human Infant. Attention and Information Processing in Infants and Adults: Perspectives from Human and Animal Research. pp. 30–60.

Richards, J. E., Conte, S. ((in press)). Brain development in infants: structure and experience. In J. J. Lockman and C. S. Tamis-LeMonda (Ed.), Cambridge Handbook of Infant Development. Cambridge University Press.

Richards, J.E., Gao, C., Conte, S., Guy, M., Xie, W., 2018. Supplemental Information for the Neural Sources of N170: Understanding Timing of Activation in Face-Selective Areas. doi:10.13140/RG.2.2.15716.01924.

Richards, J.E., Reynolds, G.D., Courage, M.L., 2010. The neural bases of infant attention. Curr. Dir. Psychol. Sci. 19 (1), 41–46. doi:10.1177/0963721409360003.

Richards, J.E., Sanchez, C., Phillips-Meek, M., Xie, W., 2015. A database of age-appropriate average MRI templates. Neuroimage doi:10.1016/j.neuroimage.2015.04.055.

Richards, J.E., Xie, W., 2015. Brains for all the ages: structural neurodevelopment in infants and children from a life-span perspective. In: Bensen, J. (Ed.), Advances in Child Development and Beahvior, 48.

Riggins, T., Scott, L.S., 2019. P300 development from infancy to adolescence. Psychophysiology e13346. doi:10.1111/psyp.13346.

Righi, G., Westerlund, A., Congdon, E.L., Troller-Renfree, S., Nelson, C.A., 2014. Infants' experience-dependent processing of male and female faces: insights from eye tracking and event-related potentials. Dev. Cogn. Neurosci. 8, 144–152. doi:10.1016/j.dcn.2013.09.005.

Rosenke, M., Weiner, K.S., Barnett, M.A., Zilles, K., Amunts, K., Goebel, R., Grill-Spector, K., 2018. A cross-validated cytoarchitectonicatlas of the human ventral visual stream. NeuroImage 170, 257–270. doi:https://doi.org/10.1016/j.neuroimage.2017.02.040.

Rossion, B., Caharel, S., 2011. ERP evidence for the speed of face categorization in the human brain: disentangling the contribution of low-level visual cues from face perception. Vis. Resour. 51 (12), 1297–1311. doi:10.1016/j.visres.2011.04.003.

Rossion, B., Gauthier, I., Tarr, M.J., Despland, P., Bruyer, R., Linotte, S., Crommelinck, M., 2000. The N170 occipito-temporal component is delayed and enhanced to inverted faces but not to inverted objects: an electrophysiological account of face-specific processes in the human brain. Neuroreport 11, 69–74.

Rossion, B., Jacques, C., 2008. Does physical interstimulus variance account for early electrophysiological face sensitive responses in the human brain? Ten lessons on the N170. Neuroimage 39 (4), 1959–1979. doi:10.1016/j.neuroimage.2007.10.011.

Rossion, B., Joyce, C.A., Cottrell, G.W., Tarr, M.J., 2003. Early lateralization and orientation tuning for face, word, and object processing in the visual cortex. Neuroimage 20 (3), 1609–1624.

Scherf, K.S., Scott, L.S., 2012. Connecting developmental trajectories: biases in face processing from infancy to adulthood. Dev. Psychobiol. 54 (6), 643–663. doi:10.1002/dev.21013.

Scott, L.S., Monesson, A., 2010. Experience-dependent neural specialization during infancy. Neuropsychologia 48 (6), 1857–1861.

Scott, L.S., Nelson, C.A., 2006. Featural and configural face processing in adults and infants: a behavioral and electrophysiological investigation. Perception 35, 1107–1128.

Scott, L.S., Shannon, R.W., Nelson, C.A., 2006. Neural correlates of human and monkey face processing in 9-month-old infants. Infancy 10 (2), 171–186.

Searle, S.R., 1987. Linear Models for Unbalanced Data. Wiley, New York, NY.

Shibata, T., Nishijo, H., Tamura, R., Miyamoto, K., Eifuku, S., Endo, S., Ono, T., 2002. Generators of visual evoked potentials for faces and eyes in the human brain as determined by dipole localization. Brain Topogr. 15 (1), 51–63.

Tottenham, N., Tanaka, J.W., Leon, A.C., McCarry, T., Nurse, M., Hare, T.A., et al., 2009. The NimStim set of facial expressions: judgments from untrained research participants. Psychiatr. Res. 168 (3), 242–249. doi:10.1016/j.psychres.2008.05.006.

Tucker, D.M., 1993. Spatial sampling of head electrical fields - the geodesic sensor net. Electroencephalogr. Clin. Neurophysiol. 87 (3), 154–163. doi:10.1016/0013-4694(93)90121-B.

Uda, S., Matsui, M., Tanaka, C., Uematsu, A., Miura, K., Kawana, I., Noguchi, K., 2015. Normal development of human brain white matter from infancy to early adulthood: a diffusion tensor imaging study. Dev. Neurosci. 37 (2), 182–194. doi:10.1159/000373885.

Webb, S.J., Long, J.D., Nelson, C.A., 2005. A longitudinal investigation of visual event-related potentials in the first year of life. Dev. Sci. 8 (6), 605–616. doi:10.1111/j.1467-7687.2005.00452.x.

Xie, W., McCormick, S.A., Westerlund, A., Bowman, L.C., Nelson, C.A., 2019. Neural correlates of facial emotion processing in infancy. Dev. Sci. 22 (3), e12758. doi:10.1111/desc.12758.

Xie, W., Richards, J.E., 2016. Effects of interstimulus intervals on behavioral, heart rate, and event-related potential indices of infant engagement and sustained attention. Psychophysiology 53 (8), 1128–1142. doi:10.1111/psyp.12670.

Xie, W., Richards, J.E., 2016. Effects of interstimulus intervals on behavioral, heart rate, and event-related potential indices of infant engagement and sustained attention. Psychophysiology 53 (8), 1128–1142. doi:10.1111/psyp.12670.